Phosphorylation of IRF4 by ROCK2 regulates IL-17 and IL-21 production and the development of autoimmunity in mice

Partha S. Biswas,[1] Sanjay Gupta,[1] Emily Chang,[1] Li Song,[1] Roslynn A. Stirzaker,[1] James K. Liao,[2] Govind Bhagat,[3] and Alessandra B. Pernis[1]

[1]Department of Medicine, Columbia University, New York, New York, USA. [2]Department of Medicine, Brigham and Women's Hospital and Harvard Medical School, Boston, Massachusetts, USA. [3]Department of Pathology, Columbia University, New York, New York, USA.

Deregulated production of IL-17 and IL-21 plays a key pathogenic role in many autoimmune disorders. A delineation of the mechanisms that underlie the inappropriate synthesis of IL-17 and IL-21 in autoimmune diseases can thus provide important insights into potential therapies for these disorders. Here we have shown that the serine-threonine kinase Rho-associated, coiled-coil–containing protein kinase 2 (ROCK2) becomes activated in mouse T cells under Th17 skewing conditions and phosphorylates interferon regulatory factor 4 (IRF4), a transcription factor that is absolutely required for the production of IL-17 and IL-21. We furthermore demonstrated that ROCK2-mediated phosphorylation of IRF4 regulated the synthesis of IL-17 and IL-21 and the differentiation of Th17 cells. Whereas CD4$^+$ T cells from WT mice activated ROCK2 physiologically under Th17 conditions, CD4$^+$ T cells from 2 different mouse models of spontaneous autoimmunity aberrantly activated ROCK2 under neutral conditions. Moreover, administration of ROCK inhibitors ameliorated the deregulated production of IL-17 and IL-21 and the inflammatory and autoantibody responses observed in these autoimmune mice. Our findings thus uncover a crucial link among ROCK2, IRF4, and the production of IL-17 and IL-21 and support the idea that selective inhibition of ROCK2 could represent an important therapeutic regimen for the treatment of autoimmune disorders.

Introduction

Accumulating evidence from murine and human studies supports a key role for IL-17 and IL-21 in the pathogenesis of several autoimmune disorders, such as RA and SLE (1–5). The molecular mechanisms that underlie the production of IL-17 and IL-21 are being rapidly elucidated (6–10). In particular, studies have demonstrated that interferon regulatory factor 4 (IRF4), a member of the IRF family of transcription factors, plays a unique and integral role in the control of these 2 cytokines since it is absolutely required for the production of both IL-17 and IL-21 (11–13). Interestingly, the expression of IRF4 is upregulated upon T cell activation and is thus not restricted to Th17 cells (14). Consistent with this finding, IRF4 regulates the function of other Th subsets, including that of Th2 cells, where it controls the production of not only IL-4, but also IL-10 and IL-21 (13, 15, 16). While the activity of other IRF family members can be regulated by serine phosphorylation (17), it is unknown whether kinases can modulate the function of IRF4. Given the pathogenic role of IL-17 and IL-21 in autoimmunity, identification of these kinases could have important biological and therapeutic implications.

During a search for regulatory proteins interacting with IRF4, our laboratory previously isolated a protein that we termed IRF4-binding protein (IBP), which is also known as SLAT; the current official term is differentially expressed in FDCP 6 (*Def6*; refs. 18–20). Def6 exerts an important immunoregulatory role in vivo, as demonstrated by the finding that Def6-deficient mice can spontaneously develop either a lupus-like syndrome or, when crossed with mice carrying the specific TCR transgene DO11.10, RA-like arthritis and vasculitis (13, 21). The autoimmune disorders that develop in the absence of Def6 are characterized by deregulated production of IL-17 and IL-21, which is due to the unrestrained ability of IRF4 to target the regulatory regions of IL-17 and IL-21 (13).

In addition to directly controlling IRF4, Def6 can also function as an activator for Rac (22, 23), a member of the Rho family of GTPases (24, 25), and lack of Def6 results in defective activation of Rac in mature CD4$^+$ T cells (21). Interestingly, extensive cross-talk exists amongst different Rho GTPases (26). In particular, Rac and RhoA can antagonize each other, since Rac activation inhibits RhoA activity and vice versa. Consistent with this notion, lack of SWAP-70, the only other protein sharing a high degree of homology with Def6 (18, 20), was recently shown to result in increased RhoA activation in dendritic cells (27). This finding led to the suggestion that this small family of proteins may control the antagonistic interaction between Rac and RhoA.

One of the major mechanisms by which activated RhoA can exert its biologic effects is by binding to and activating the Rho-associated, coiled-coil–containing protein kinases (ROCKs). ROCKs are serine/threonine kinases that include 2 isoforms, ROCK1 and ROCK2, encoded by 2 different genes (28–31). Consistent with their role in the regulation of cytoskeletal reorganization, ROCKs have been shown to regulate the migration of CD4$^+$ T cells (32, 33). Interestingly, increased ROCK activity has been observed in CD4$^+$ T cells from SLE patients, and ROCK inhibitors have been shown to ameliorate the cytoskeletal abnormalities exhibited by T cells from SLE patients (34). In addition to its effects on the T cell cytoskeleton, ROCKs may also play a role in the activation of CD4$^+$ T cells, as suggested by the finding that ROCK inhibitors can decrease the production of cytokines such as IL-2 and IFN-γ by naive T cells (35). Intriguingly, however, these inhibitors did not

Conflict of interest: The authors have declared that no conflict of interest exists.
Citation for this article: *J Clin Invest.* 2010;120(9):3280–3295. doi:10.1172/JCI42856.

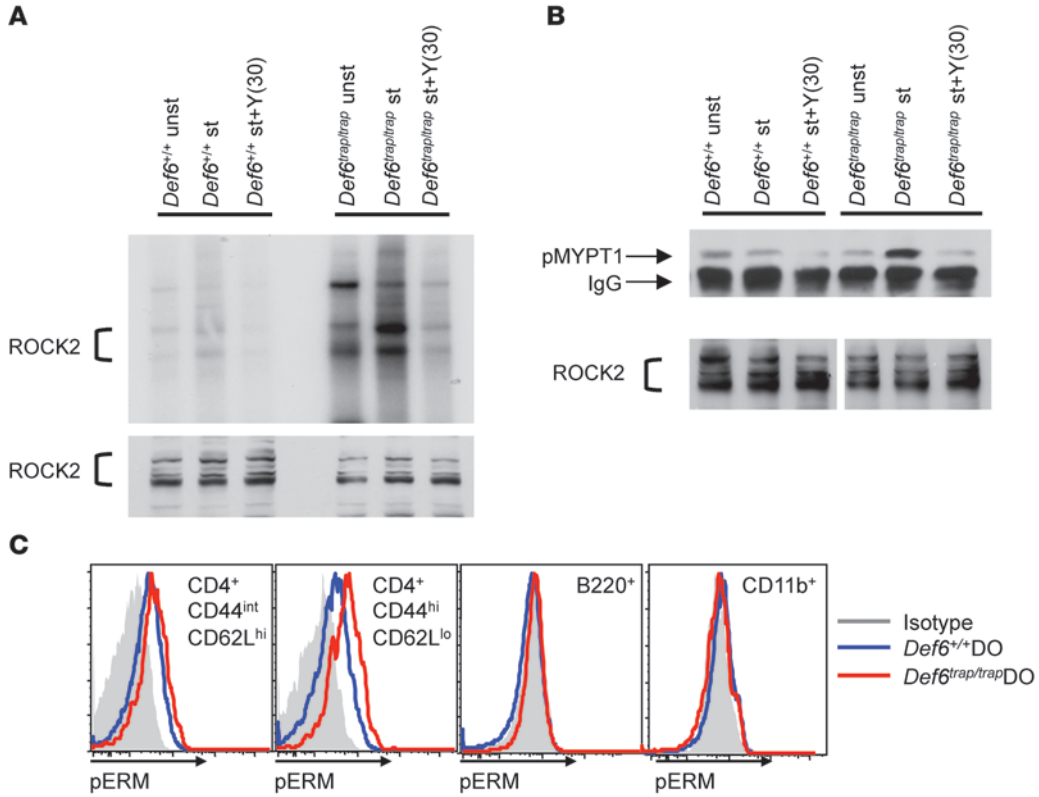

Figure 1
Enhanced ROCK2 activation in the absence of Def6. (**A** and **B**) Purified CD4+ T cells from *Def6*$^{+/+}$ or *Def6*$^{trap/trap}$ mice were either left unstimulated (unst) or restimulated (st) with anti-CD3 and anti-CD28 mAbs for 48 hours in the presence or absence of 30 μM Y27632 [Y(30)]. (**A**) ROCK2 kinase activity was measured by in vitro kinase assay using [γ-^{32}P]ATP. Autophosphorylated ROCK2 was detected by autoradiography. (**B**) ROCK2 kinase activity was assayed by incubating immunoprecipitated ROCK2 with purified rMYPT1 as ROCK2 substrate, and pMYPT1 was detected by Western blot analysis using anti-pMYPT1 Ab. In **A** and **B**, total ROCK2 levels in the input samples are shown below. In **B**, lanes were run on the same gel but were noncontiguous (white line). (**C**) Levels of pERM in CD4$^+$CD44^{int}CD62L^{hi}, CD4$^+$CD44^{hi}CD62L^{lo}, B220$^+$, and CD11b$^+$ cells from *Def6*$^{+/+}$DO11.10 or *Def6*$^{trap/trap}$DO11.10 mice were detected by intracellular staining with anti-pERM Ab and analyzed by FACS. Solid histograms indicate isotype control. Shown are overlaid histograms after gating on the appropriate populations. (**A**–**C**) Data are representative of 3 independent experiments.

alter the production of these cytokines by primed CD4$^+$ T cells (35). The precise role of ROCKs in the function of effector CD4$^+$ T cells has not been delineated.

Given the ability of Def6 to activate Rac and the known antagonism between Rac- and RhoA-mediated pathways, we investigated whether lack of Def6 would lead to enhanced activation of ROCKs in CD4$^+$ T cells. We demonstrated that WT CD4$^+$ T cells activated ROCK2 when exposed to Th17, but not Th0, conditions. We furthermore showed that activated ROCK2 regulated the production of IL-17 and IL-21 as a result of its ability to phosphorylate IRF4. In contrast to WT T cells, Def6-deficient CD4$^+$ T cells aberrantly activated ROCK2 under neutral conditions. Aberrant ROCK2 activation was also detected in CD4$^+$ T cells from another spontaneous mouse model of autoimmunity, the lupus-prone MRL/lpr mouse. Administration of ROCK inhibitors to either Def6-deficient or MRL/lpr mice decreased the production of IL-17 and IL-21 and ameliorated the autoimmune symptoms that spontaneously develop in these mice. We therefore propose that ROCK2-mediated phosphorylation of IRF4 is a novel regulatory step controlling the production of IL-17 and IL-21 and that aberrant activation of ROCK2 in CD4$^+$ T cells may play a pathogenic role in autoimmunity.

Results

Lack of Def6 leads to increased ROCK2 activity in CD4$^+$ T cells. Although ROCKs have been extensively characterized in endothelial cells and other nonhematopoietic cells, to our knowledge, their expression in CD4$^+$ T cells has not been examined. Interestingly, we found that T cell activation led to downregulation of ROCK1 expression, but did not significantly affect the expression of ROCK2 (Supplemental Figure 1, A and B; supplemental material available online with this article; doi:10.1172/JCI42856DS1), which indicates that ROCK2 is the major ROCK isoform present in activated CD4$^+$ T cells.

To directly investigate whether the absence of Def6 alters ROCK2 activity in CD4$^+$ T cells, in vitro kinase activity assays were performed. Lack of Def6 markedly increased the autophosphorylation of ROCK2 upon T cell stimulation, and this effect was blocked by addition of Y27632 (Figure 1A), a well-known ROCK inhibitor (36, 37). These findings were further corroborated by assaying the ability of immunoprecipitated ROCK2 to phosphorylate recombinant MYPT1 (rMYPT1), a known ROCK substrate (38). Consistent with the in vitro kinase assay, ROCK2 immunoprecipitates from stimulated Def6-deficient CD4$^+$ T cells exhibited higher levels of phosphorylated MYPT1 (pMYPT1) than did ROCK2 immunoprecipitates from stimulated *Def6*$^{+/+}$ CD4$^+$ T

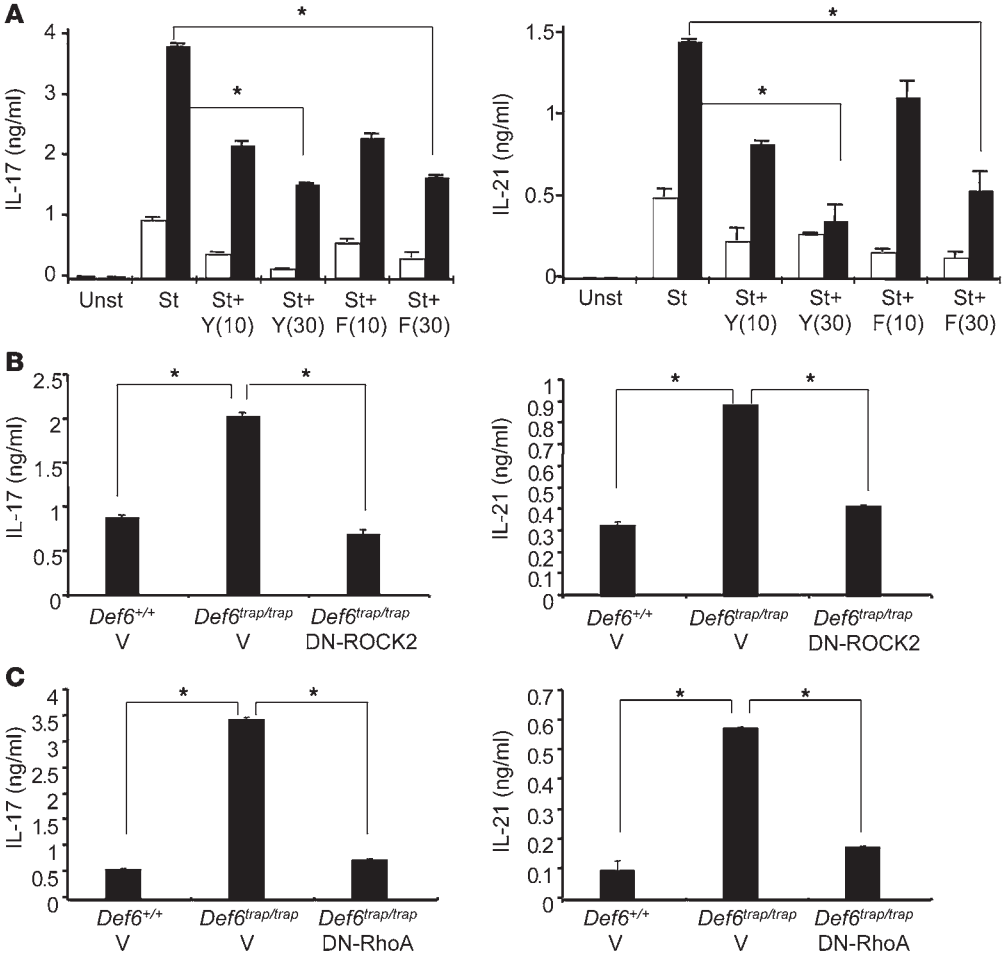

Figure 2

ROCK2 inhibition ameliorates aberrant production of IL-17 and IL-21 by Def6-deficient CD4+ T cells. (**A**) Purified CD4+ T cells from *Def6*$^{+/+}$DO11.10 (white bars) or *Def6*$^{trap/trap}$DO11.10 (black bars) mice were either left unstimulated or restimulated with anti-CD3 and anti-CD28 mAbs for 48 hours in the presence or absence of 10 or 30 μM Y27632 or Fasudil. Supernatants were then collected and assayed for IL-17 and IL-21 production by ELISA. Data are representative of 3 independent experiments. **P* ≤ 0.03. (**B**) CD4+ T cells from *Def6*$^{+/+}$ or *Def6*$^{trap/trap}$ mice were infected with control YFP-RV or DN-ROCK2–expressing retroviruses. Cells were harvested after 6 days, sorted for YFP+ cells, and restimulated with anti-CD3 and anti-CD28 for 48 hours. Supernatants were then collected and assayed for IL-17 and IL-21 production by ELISA. Data are representative of 3 independent experiments. V, vector control. **P* ≤ 0.01. (**C**) CD4+ T cells from *Def6*$^{+/+}$ or *Def6*$^{trap/trap}$ mice were infected with control GFP-RV or DN-RhoA–expressing retroviruses. Cells were harvested after 6 days, sorted for GFP+ cells, and restimulated with anti-CD3 and anti-CD28 for 48 hours. Supernatants were then collected and assayed for IL-17 and IL-21 production by ELISA. V, vector control. Data are representative of 3 independent experiments. **P* ≤ 0.0002.

cells, an effect that was inhibited by Y27632 (Figure 1B). Because phosphorylation of ezrin/radixin/moesin proteins (pERM) is also used to gauge ROCK activity (39), we detected pERM proteins by intracellular FACS in mice lacking Def6. Increased pERM was clearly observed in CD44^{hi}CD62L^{lo}CD4+ T cells derived from Def6-deficient mice, regardless of the presence of the DO11.10 transgene (Figure 1C and Supplemental Figure 1C). Enhancement in pERM was restricted to the T cell compartment, since it was not observed in B cells or myeloid cells (Figure 1C). Taken together, these data suggest that lack of Def6 causes increased ROCK2 activation in CD4+ T cells stimulated under neutral conditions.

Inhibition of ROCK2 decreases production of IL-17 and IL-21 by Def6-deficient CD4+ T cells. Although the majority of known ROCK2 targets are cytoskeletal proteins, ROCK2 can also be detected in the nucleus (ref. 40 and Supplemental Figure 1B). We thus investigated whether aberrant activation of ROCK2 contributes to the deregulated expression of IL-17 and IL-21 that characterizes Def6-deficient CD4+ T cells (13). To evaluate this possibility, we first explored the effects of 2 distinct ROCK inhibitors, Y27632 and Fasudil (36, 37), on the production of IL-17 and IL-21 by Def6-deficient CD4+ T cells. Given that the abnormalities in pERM were primarily observed within the effector/memory CD4+ T cell compartment, the experiments were conducted on CD4+ T cells subjected to a first round of stimulation under neutral conditions and then restimulated. Y27632 and Fasudil interfered with the enhanced production of IL-17 and IL-21 by Def6-deficient DO11.10 (referred to herein as *Def6*$^{trap/trap}$DO11.10; see Methods) CD4+ T cells in a dose-dependent manner (Figure 2A). ROCK inhibition, however, did not alter the ability of *Def6*$^{trap/trap}$DO11.10 CD4+ T cells to produce IL-4 and IL-10, 2 cytokines known to be regulated by IRF4 (15, 16, 41), or correct their defects in IL-2 and IFN-γ synthesis

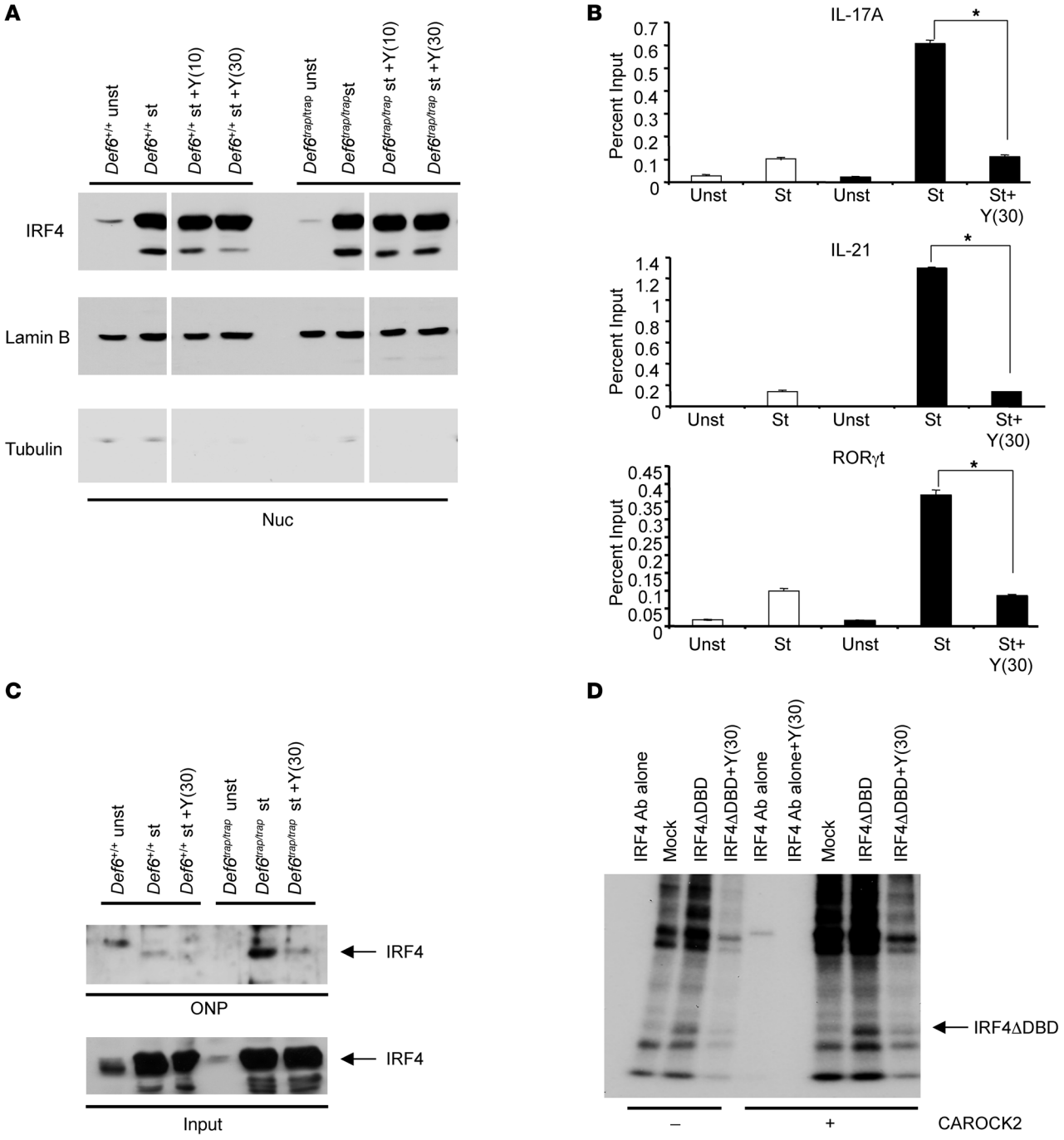

Figure 3

ROCK2 can directly phosphorylate IRF4. (**A**–**C**) CD4+ T cells were purified from *Def6*$^{+/+}$ or *Def6*$^{trap/trap}$ mice and left unstimulated or restimulated for 48 hours with anti-CD3 and anti-CD28 Abs in the presence or absence of Y27632. (**A**) Nuclear extracts were analyzed by Western blotting using an IRF4 Ab; the blot was later stripped and reprobed with a Lamin B Ab or with a tubulin Ab to ensure for equivalent loading and purity of the fractions. Lanes were run on the same gel but were noncontiguous (white lines). (**B**) ChIP assays were carried out with IRF4 or control Ab. Quantification of IRF4 binding to the IL-17A, IL-21, and RORγt promoters was performed using quantitative PCR. White bars, *Def6*$^{+/+}$; black bars, *Def6*$^{trap/trap}$. *$P \leq 0.004$. (**C**) Nuclear extracts were prepared and subjected to ONP assay (see Methods). Precipitated proteins were analyzed by Western blotting with an IRF4 Ab; IRF4 levels in the input extracts are shown below. (**D**) 293T cells were transiently transfected with empty vector (mock) or with an expression vector for IRF4ΔDBD mutant. Whole cell lysates were then prepared and immunoprecipitated with an IRF4 Ab. Immunoprecipitates were subjected to in vitro kinase reactions with or without purified CAROCK2 in the presence of [γ-^{32}P]ATP. Y27632 was added in selected reaction samples as indicated. Reaction samples were resolved by 10% SDS-PAGE, and phosphorylated products were subsequently detected by autoradiography. Data are representative of 2 (**B** and **D**) or 3 (**A** and **C**) independent experiments.

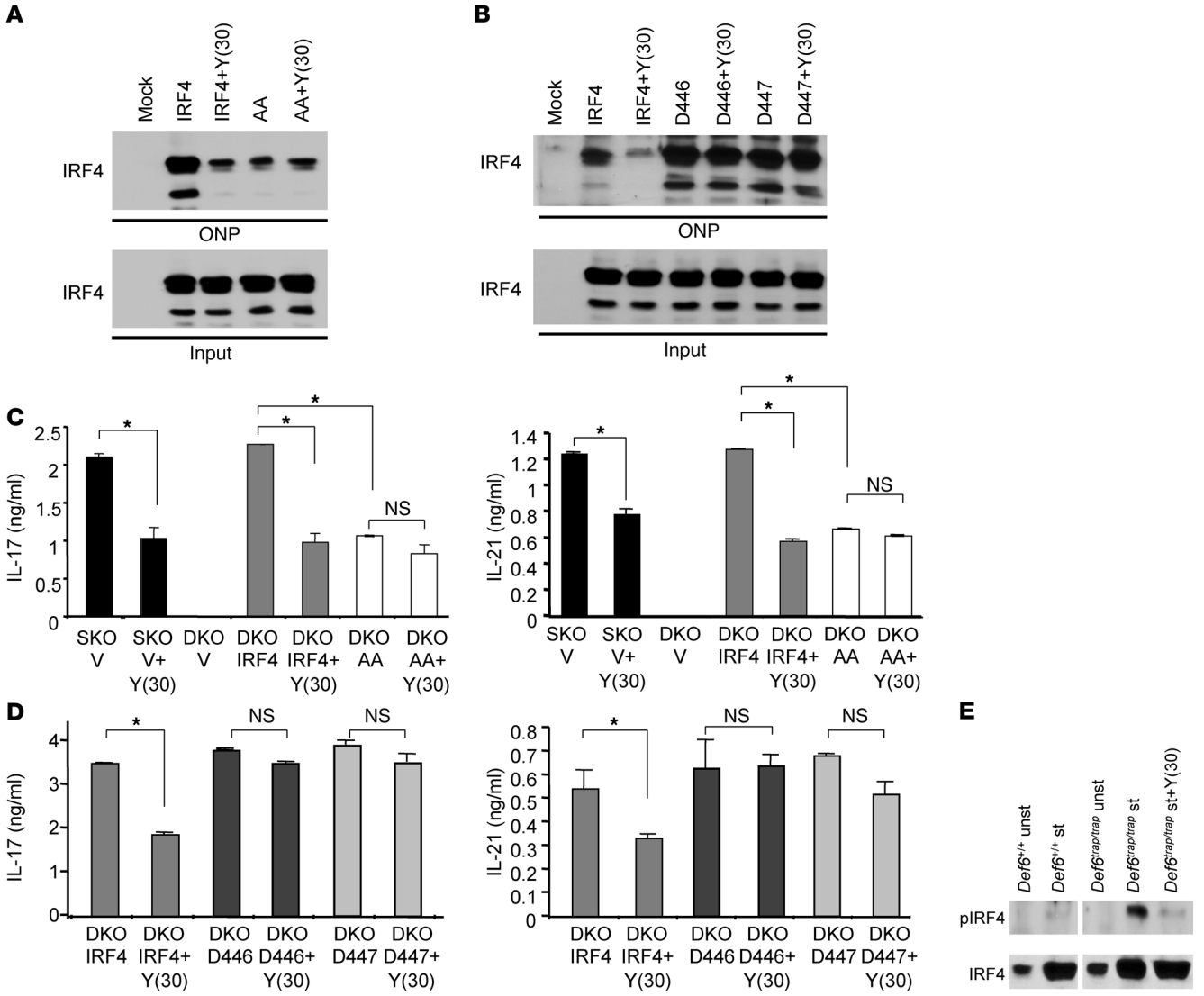

Figure 4

Role of S446 and S447 of IRF4 in IL-17 and IL-21 production. (**A** and **B**) ONP assay was performed on nuclear extracts from 293T cells transfected with empty vector or expression vector for WT IRF4 and (**A**) IRF4AA or (**B**) IRF4D446 or IRF4D447. Y27632 was added in selected cultures as indicated. Precipitated proteins were analyzed by Western blotting with IRF4 Ab; IRF4 levels in the input samples are shown below. (**C** and **D**) CD4$^+$ T cells from *Def6*$^{trap/trap}$ single-KO (SKO) and *Def6*$^{trap/trap}$*Irf4*$^{-/-}$ double-KO (DKO) mice were infected with control YFP-RV (V), WT IRF4, and IRF4 mutants-expressing retroviruses as indicated. Cells were harvested after 6 days, sorted for YFP$^+$ cells, and restimulated with anti-CD3 and anti-CD28 for 48 hours in the presence or absence of 30 μM Y27632. Supernatants were then collected and assayed for IL-17 and IL-21 production by ELISA. *$P \leq 0.004$. (**E**) CD4$^+$ T cells purified from *Def6*$^{+/+}$ and *Def6*$^{trap/trap}$ were stimulated as described in Figure 3. Nuclear extracts were analyzed by Western blotting using an Ab that recognizes pIRF4. The blot was later stripped and reprobed with an Ab against total IRF4. Lanes were run on the same gel but were noncontiguous (white lines). Data are representative of 3 independent experiments (**A**–**E**).

(Supplemental Figure 2A). Y27632 and Fasudil also inhibited IL-17 and IL-21 protein and transcript levels by *Def6*$^{trap/trap}$ CD4$^+$ T cells lacking the DO11.10 transgene (Supplemental Figure 2, B and C). The increased expression of RORγt observed in the absence of Def6 (13) was also ameliorated by ROCK inhibition (Supplemental Figure 2C). Together, these findings indicate that ROCK inhibitors can selectively ameliorate the aberrant production of IL-17 and IL-21 by Def6-deficient CD4$^+$ T cells.

To ensure that the suppressive effects of the ROCK inhibitors on IL-17 and IL-21 production were indeed caused by activation of the RhoA-ROCK2 pathway, *Def6*$^{trap/trap}$ CD4$^+$ T cells were stimulated under neutral conditions and transduced with a vector control or with a construct expressing a dominant-negative form of ROCK2 (DN-ROCK2; ref. 42) or of RhoA (DN-RhoA; refs. 43, 44). Expression of DN-ROCK2 or DN-RhoA markedly inhibited the increased production of IL-17 and IL-21 by Def6-deficient CD4$^+$ T cells (Figure 2, B and C). This effect was selective for IL-17 and IL-21, since expression of DN-ROCK2 and DN-RhoA had no effect on the production of IL-10 by Def6-deficient CD4$^+$ T cells (Supplemental Figure 2, D and E). These results thus confirmed that the lack of Def6 led to increased activation of the RhoA-ROCK2 pathway in CD4$^+$ T cells and that targeting this

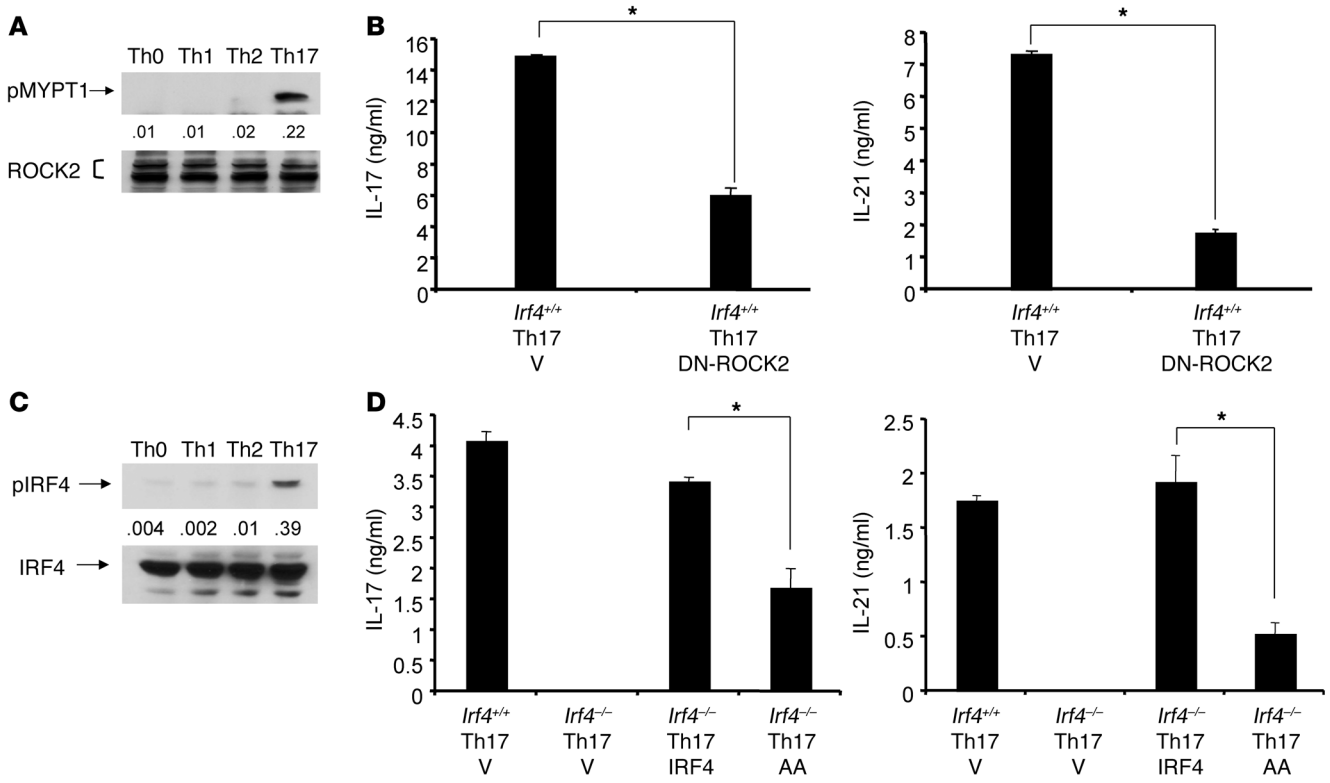

Figure 5

ROCK2 is activated under Th17 skewing conditions and regulates IRF4 function during Th17 differentiation. (**A**) Sorted naive ($CD44^{lo}CD62L^{hi}CD25^{-}$) $CD4^{+}$ T cells from *Irf4*$^{+/+}$ mice were stimulated under Th0, Th1, Th2, or Th17 skewing conditions (TGF-β plus IL-6) for 5 days. ROCK2 kinase activity was assayed by incubating the immunoprecipitated ROCK2 with purified rMYPT1 as ROCK2 substrate. pMYPT1 was detected by Western blot analysis using anti-pMYPT1 Ab; total ROCK2 levels in the input samples are shown below. Numbers denote ratio of pMYPT1/total ROCK2 integrated density, measured by ImageJ. (**B**) Sorted naive $CD4^{+}$ T cells from *Irf4*$^{+/+}$ mice were infected with control YFP-RV or DN-ROCK2–expressing retroviruses and stimulated under Th17 skewing conditions. Cells were harvested after 5 days, sorted for YFP^{+} cells, and restimulated with anti-CD3 and anti-CD28 for 48 hours. Supernatants were collected and assayed for IL-17 and IL-21 production by ELISA. $^{*}P \leq 0.001$. (**C**) Sorted naive $CD4^{+}$ T cells from *Irf4*$^{+/+}$ mice were stimulated under the indicated conditions for 3 days. Nuclear extracts were analyzed by Western blotting using an Ab that recognizes pIRF4; the blot was later stripped and reprobed with an Ab against total IRF4. Numbers denote ratio of pIRF4/total IRF4 integrated density, measured by ImageJ. (**D**) Sorted naive $CD4^{+}$ T cells from *Irf4*$^{-/-}$ mice were infected with control YFP-RV, WT IRF4, or IRF4AA-expressing retroviruses and stimulated under Th17 skewing conditions. Cells were harvested, sorted, and restimulated, and supernatants collected and assayed, as in **B**. $^{*}P \leq 0.02$. Data in **A**–**D** are representative of 3 independent experiments.

pathway ameliorated the aberrant production of IL-17 and IL-21 observed in the absence of Def6.

ROCK2 phosphorylates IRF4 and controls its ability to bind to the IL-17 and IL-21 promoters. The finding that ROCK inhibitors were able to modulate the synthesis of both IL-17 and IL-21 suggested that ROCK2 might control the function of IRF4, since this transcription factor plays an integral role in the regulation of both IL-17 and IL-21 (11–13). We first investigated whether addition of Y27632 alters the expression of IRF4. Neither induction of IRF4 upon T cell stimulation nor nuclear localization of IRF4 was affected by addition of Y27632 to the cultures (Figure 3A). However, the presence of Y27632 inhibited aberrant binding of IRF4 to the IL-17A, IL-21, and RORγt promoters, which was observed in Def6-deficient $CD4^{+}$ T cells by ChIP experiments and by oligonucleotide precipitation (ONP) assays (Figure 3, B and C). These findings thus suggest that ROCK2 regulates the ability of IRF4 to bind to the IL-17, IL-21, and RORγt promoters.

Because a survey of the IRF4 sequence revealed the presence of potential ROCK2 phosphorylation sites within its carboxy terminus, we next performed an in vitro kinase assay to assess whether IRF4 itself is directly phosphorylated by ROCK2. Since IRF4 is a 50-kDa protein, we sought to avoid overlap with the heavy chain of the precipitating Ab by using a deletion mutant of IRF4 that lacks the aminoterminal DNA binding domain (IRF4ΔDBD) and runs as an approximately 35-kDa protein band. Extracts from 293T cells transfected with the IRF4ΔDBD mutant were immunoprecipitated with an IRF4 Ab and then incubated with [γ^{32}P] ATP in the presence or absence of purified constitutively active ROCK2 (CAROCK2). In the absence of CAROCK2, low-level phosphorylation of IRF4ΔDBD was detected (Figure 3D). This effect was likely caused by baseline activation of endogenous ROCK2 in 293T cells grown in serum (45), because it was blocked by Y27632. Phosphorylation of IRF4ΔDBD was markedly augmented by the addition of CAROCK2, an effect that was inhibited by Y27632. Mass spectrometry analysis confirmed that CAROCK2 phosphorylated IRF4 at either of 2 distinct phosphorylation sites, S446 and S447, which are located carboxy-terminal to the IRF association domain (Supplemental Figure 3, A and B). Thus, IRF4 was directly phosphorylated by ROCK2.

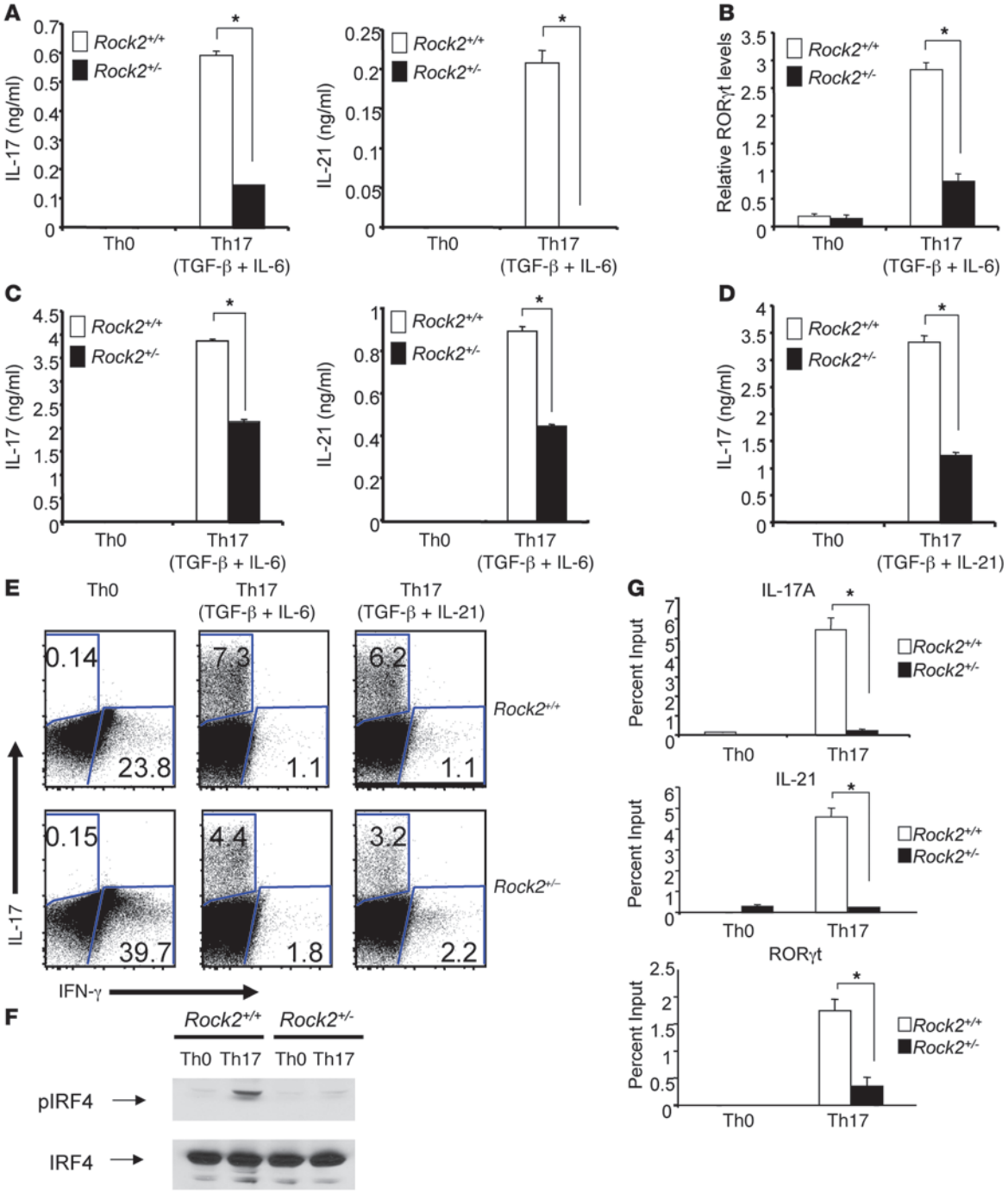

Figure 6

ROCK2 haploinsufficiency impairs Th17 differentiation. (**A**) Sorted naive CD4+ T cells from either *Rock2*$^{+/+}$ or *Rock2*$^{+/-}$ mice were stimulated under either Th0 or Th17 (TGF-β + IL-6) for 3 days. IL-17 and IL-21 production was determined by ELISA. *$P \leq 0.0005$. (**B**) Sorted naive CD4+ T cells were stimulated as in **A**. Relative expression of RORγt mRNA was quantified using quantitative PCR. *$P = 0.001$. (**C**) Sorted naive CD4+ T cells from either *Rock2*$^{+/+}$ or *Rock2*$^{+/-}$ mice were stimulated under either Th0 or Th17 (TGF-β + IL-6) conditions for 5 days. IL-17 and IL-21 production was determined by ELISA. *$P \leq 0.0009$. (**D**) Sorted naive CD4+ T cells from either *Rock2*$^{+/+}$ or *Rock2*$^{+/-}$ mice were stimulated under either Th0 or Th17 (TGF-β + IL-21) cell conditions for 5 days. IL-17 production was determined by ELISA. *$P = 0.007$. (**E**) Sorted naive CD4+ T cells from either *Rock2*$^{+/+}$ or *Rock2*$^{+/-}$ mice were stimulated under either Th0 or Th17 (IL-6 + TGF-β + or IL-21 + TGF-β) conditions for 5 days. After restimulation with PMA/Ionomycin, intracellular staining for IL-17 and IFN-γ was performed. (**F**) Sorted naive CD4+ T cells from *Rock2*$^{+/+}$ and *Rock2*$^{+/-}$ mice were stimulated as in **A**. Nuclear extracts were analyzed by Western blotting as in Figure 4E. (**G**) Sorted naive CD4+ T cells from either *Rock2*$^{+/+}$ or *Rock2*$^{+/-}$ mice cultured as in **A** were subjected to ChIP assays with either IRF4 or control Ab. Quantification of IRF4 binding to the IL-17A, IL-21, and RORγt promoters was performed using quantitative PCR. *$P \leq 0.01$. Data are representative of 2 (**B**, **F**, and **G**) or 3 (**A**, **C**, **D**, and **E**) independent experiments.

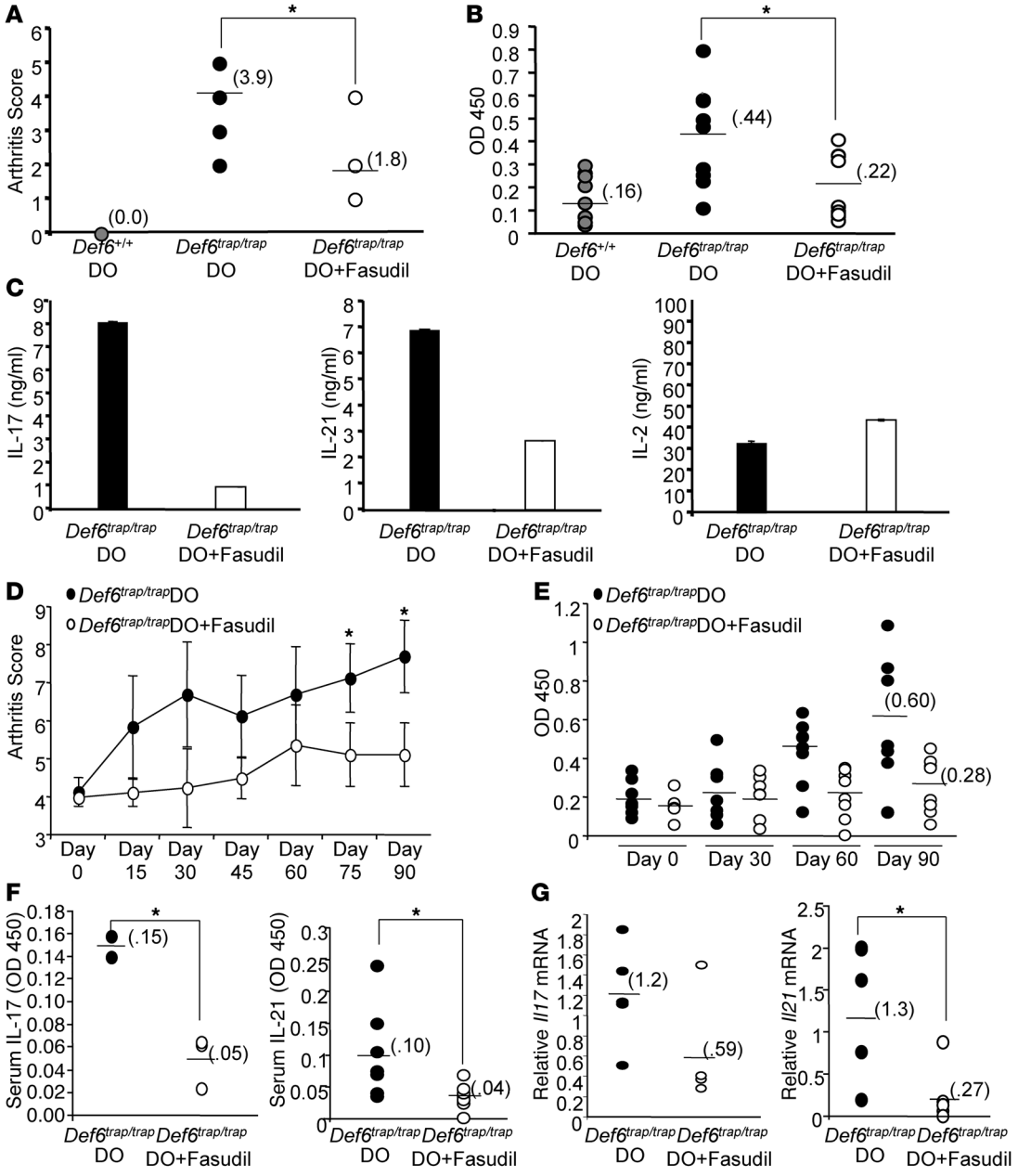

Figure 7

ROCK inhibition decreases IL-17 and IL-21 production in vivo and ameliorates arthritis development in *Def6*$^{trap/trap}$DO11.10 mice. (**A** and **B**) Prevention protocol. *Def6*$^{trap/trap}$DO11.10 mice were treated or not with Fasudil starting at 8 weeks of age; *Def6*$^{+/+}$DO11.10 mice were controls (n = 10 per group). (**A**) Arthritis severity, assessed by histological score. *P = 0.0001. (**B**) Sera were collected, and RF levels were analyzed by ELISA. *P = 0.01. (**C**) CD4$^+$ T cells were harvested from *Def6*$^{trap/trap}$DO11.10 mice treated or not with Fasudil, restimulated in vitro with anti-CD3 and anti-CD28, and assessed for IL-17, IL-21, and IL-2 production by ELISA. (**D**–**G**) Treatment protocol. *Def6*$^{trap/trap}$DO11.10 mice were treated or not with Fasudil (n = 8 and 7, respectively, unless otherwise indicated) starting at 14 weeks of age. (**D**) Arthritis severity, assessed by histological score. *$P \leq 0.008$. (**E** and **F**) Sera were collected, and levels of RF (**E**) as well as IL-17 (n = 3 per group) and IL-21 (**F**) were analyzed by ELISA. *$P \leq 0.04$. (**G**) Joints were collected, and *Il17* and *Il21* gene expression was analyzed by real-time RT-PCR. *P = 0.03. (**A**, **B**, and **D**–**G**) Circles represent individual mice; bars and parenthetical values denote group means.

To investigate whether phosphorylation by ROCK2 regulates the activity of IRF4, we generated an IRF4 mutant in which both S446 and S447 were mutated to alanines (IRF4AA). We examined its ability to bind to DNA by ONP assay; binding of the IRF4AA mutant to the IRF4 binding site from the IL-21 promoter was greatly diminished compared with that of WT IRF4 (Figure 4A). Furthermore, whereas binding of WT IRF4 was decreased by culturing in the presence of Y27632, binding of IRF4AA was unaffected by the presence of the ROCK inhibitor. We next examined the effects of mutating either S446 or S447 to aspartic acid, thus

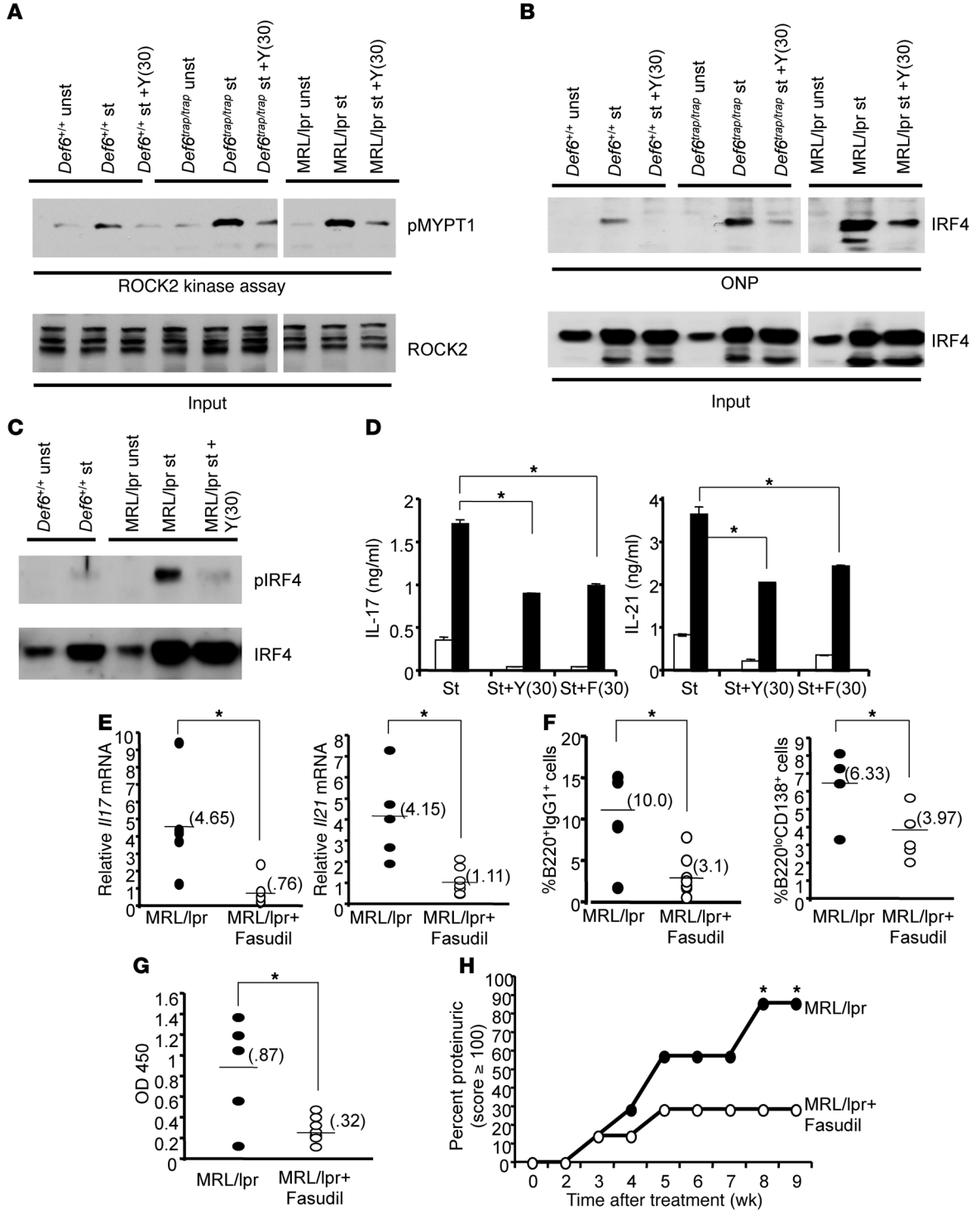
A
Def6+/+ unst
Def6+/+ st
Def6+/+ st +Y(30)
Def6trap/trap unst
Def6trap/trap st
Def6trap/trap st +Y(30)
MRL/lpr unst
MRL/lpr st
MRL/lpr st +Y(30)
pMYPT1
ROCK2 kinase assay
ROCK2
Input
B
IRF4
ONP
IRF4
Input
C
pIRF4
IRF4
D
IL-17 (ng/ml)
IL-21 (ng/ml)
St
St+Y(30)
St+F(30)
E
Relative Il17 mRNA
Relative Il21 mRNA
(4.65)
(.76)
(4.15)
(1.11)
MRL/lpr
MRL/lpr+ Fasudil
F
%B220+IgG1+ cells
%B220loCD138+ cells
(10.0)
(3.1)
(6.33)
(3.97)
G
OD 450
(.87)
(.32)
H
Percent proteinuric (score ≥ 100)
MRL/lpr
MRL/lpr+ Fasudil
Time after treatment (wk)

Figure 8
Enhanced ROCK2 activation and aberrant IRF4 function in MRL/lpr CD4+ T cells. (**A**–**C**) CD4+ T cells were purified from *Def6*$^{+/+}$, *Def6*$^{trap/trap}$, and MRL/lpr mice, subjected to primary stimulation, and left unstimulated or restimulated for 48 hours with anti-CD3 and anti-CD28 Abs in the presence or absence of Y27632. (**A**) ROCK2 kinase activity was assayed as in Figure 1B, with total ROCK2 levels in the input samples shown below. (**B**) Cells were subjected to ONP assay as in Figure 3C. Lanes in **A** and **B** were run on the same gel but were noncontiguous (white lines). (**C**) Nuclear extracts were analyzed by Western blotting as in Figure 6F. (**D**) Purified CD4+ T cells from Balb/c (white bars) and MRL/lpr (black bars) mice were stimulated as in **A**. Supernatants were then collected and assayed for IL-17 and IL-21 production by ELISA. *$P \leq 0.04$. Data in **A**–**D** are representative of 3 independent experiments. (**E**–**H**) MRL/lpr mice were treated or not with Fasudil ($n = 7$ per group, unless otherwise indicated). (**E**) Spleens were collected, and IL-17 and IL-21 gene expression was analyzed by real-time RT-PCR ($n = 5$, untreated MRL/lpr). *$P \leq 0.04$. (**F**) Percentages of splenic B220+sIgG1+ and B220^{lo}CD138+ cells. *$P \leq 0.04$. (**G**) Serum levels of anti-dsDNA Abs, analyzed by ELISA. *$P = 0.02$. In **E**–**G**, circles represent individual mice; bars and parenthetical values denote group means. (**H**) Proteinuria over 9 weeks of treatment beginning at 10 weeks of age. *$P \leq 0.02$, 2-tailed Mann Whitney *U* test.

generating the phosphomimetic forms IRF4D446 and IRF4D447, respectively. The IRF4D446 and IRF4D447 mutants demonstrated stronger binding to this DNA site than did WT IRF4 (Figure 4B). Importantly, binding of the IRF4D446 and IRF4D447 mutants to this site was completely resistant to the inhibitory effects of Y27632 (Figure 4B). These findings thus indicate that phosphorylation of IRF4 by ROCK2 on S446 or S447 can regulate its ability to bind DNA.

To further assess the functional consequences of ROCK2-mediated IRF4 phosphorylation, retroviral transduction experiments were conducted using CD4+ T cells from mice deficient in both Def6 and IRF4. Concurrent deletion of IRF4 completely abolishes IL-17 and IL-21 synthesis by CD4+ T cells lacking Def6 (13), enabling us to directly assess the contribution of IRF4 phosphorylation to the abnormal cytokine production by these cells. Reconstitution with the IRF4AA mutant led to IL-17 and IL-21 levels significantly lower than those produced by reconstitution with WT IRF4, although the 2 constructs exhibited similar transduction efficiencies (Figure 4C and Supplemental Figure 4A). Furthermore, whereas addition of Y27632 decreased WT IRF4–mediated production of IL-17 and IL-21 to levels observed with the IRF4AA mutant, the effects of the IRF4AA mutant were not altered by Y27632 (Figure 4C). Interestingly, reconstitution with the IRF4A446 and IRF4A447 mutants, in which only 1 of the 2 serines was mutated to alanine, demonstrated that mutation of S446 impaired the ability of IRF4 to mediate production of IL-17 more so than did mutation of S447 (Supplemental Figure 4B). To further extend these findings, we conducted transduction experiments with IRF4D446 and IRF4D447. Reintroduction of either rescued production of IL-17 and IL-21 to levels similar to those observed with WT IRF4 (Figure 4D and Supplemental Figure 4C). Addition of Y27632, however, inhibited the production of IL-17 and IL-21 by WT IRF4, but not that mediated by IRF4D446 or IRF4D447. Thus, phosphorylation of IRF4 at S446 or S447 altered its ability to regulate the production of IL-17 and IL-21. Although ROCK2 can phosphorylate either S446 or S447 within IRF4, S446 appears to be the preferred residue targeted by ROCK2 in primary CD4+ T cells.

The identification of the key IRF4 residues phosphorylated by ROCK2 enabled us to generate an Ab that specifically recognizes the phosphorylated form of IRF4 (pIRF4). The Ab did not detect either WT IRF4 or the IRF4AA mutant, but strongly recognized the IRF4D446 mutant (Supplemental Figure 4D). Notably, probing of nuclear extracts from CD4+ T cells with the pIRF4 Ab clearly revealed the presence of pIRF4 in stimulated Def6-deficient, but not WT, CD4+ T cells (Figure 4E). As predicted, pIRF4 was not detected in Def6-deficient CD4+ T cells when these cells were stimulated in the presence of Y27632 (Figure 4E). In addition, the pIRF4 Ab successfully detected phosphorylation of IRF4ΔDBD after in vitro kinase reaction with CAROCK2 (Supplemental Figure 4E). Together, these observations support the notion that ROCK2-mediated IRF4 phosphorylation regulates expression of IL-17 and IL-21 by CD4+ T cells.

ROCK2 is activated under Th17 skewing conditions in WT CD4+ T cells and regulates Th17 differentiation. TGF-β is known to activate the RhoA-ROCK pathway in nonhematopoietic cells (46). Because TGF-β controls the differentiation of Th17 cells (6–10), we next explored the possibility that ROCK2 activation occurs physiologically when CD4+ T cells from nonautoimmune mice are exposed to Th17 skewing conditions. Naive CD4+ T cells were purified from WT mice and cultured in vitro under Th0, Th1, Th2, or Th17 conditions. Extracts were then prepared, ROCK2 immunoprecipitated, and assayed for pMYPT1. ROCK2 immunoprecipitates from WT CD4+ T cells cultured under Th17 skewing conditions exhibited increased pMYPT1 compared with cells cultured under Th0 conditions (Figure 5A). Furthermore, no activation of ROCK2 under Th1 or Th2 polarizing conditions was observed. Consistent with the idea that TGF-β is the critical stimulus driving the activation of ROCK2, the presence of IL-6 alone did not lead to ROCK2 activation (Supplemental Figure 5A). Thus, the presence of a specific cytokine milieu was required for normal activation of ROCK2 in CD4+ T cells from WT mice.

The finding that ROCK2 was normally activated under Th17 conditions raised the possibility that ROCK2 activation plays a physiological role in Th17 differentiation. To explore this notion, naive CD4+ T cells from WT mice were stimulated under Th17 conditions and transduced with a vector control or with a construct expressing DN-ROCK2. Expression of DN-ROCK2 markedly inhibited the production of IL-17 and IL-21 by WT CD4+ T cells grown under Th17 conditions (Figure 5B), which suggests that activation of ROCK2 plays an important role in Th17 differentiation.

To evaluate whether activation of ROCK2 in WT CD4+ T cells exposed to Th17 conditions results in IRF4 phosphorylation, we used the Ab we generated against pIRF4. Western blotting of nuclear extracts derived from naive WT CD4+ T cells differentiated under Th0, Th1, Th2, or Th17 conditions revealed prominent pIRF4 only when WT CD4+ T cells were exposed to Th17 skewing conditions (Figure 5C). To directly assess the functional importance of IRF4 phosphorylation in the differentiation of Th17 cells, we compared the ability of WT IRF4 and IRF4AA to rescue Th17 differentiation in *Irf4*$^{-/-}$ CD4+ T cells. As previously reported (11–13), *Irf4*$^{-/-}$ CD4+ T cells exposed to Th17 polarizing conditions completely lacked the ability to produce IL-17 and IL-21 (Figure 5D). Reintroduction of WT IRF4 restored IL-17 and IL-21 production to levels comparable to those exhibited by *Irf4*$^{+/+}$ CD4+ T cells. In contrast, despite similar transduction efficiency (Supplemental Figure 5B), IRF4AA exhibited a limited ability to rescue the production of IL-17 and IL-21. These results indicate that in WT

$CD4^+$ T cells, IRF4 becomes phosphorylated under Th17 skewing conditions, and that IRF4 phosphorylation is normally required for optimal Th17 differentiation.

To further investigate the physiologic role of ROCK2 in Th17 differentiation, we used mice haploinsufficient in ROCK2. Although complete lack of ROCK2 leads to embryonic lethality (47), haploinsufficient ROCK2 mutant mice develop normally (48), and we did not observe any major immune developmental abnormality (Supplemental Table 1). However, since activation of ROCKs involves their dimerization (49), haploinsufficiency can result in decreased ROCK2 function. Exposure of naive $CD4^+$ cells from *Rock2*$^{+/-}$ mice to Th17 skewing conditions resulted in decreased production of IL-17 and IL-21 as well as in reduced RORγt transcript levels (Figure 6, A and B). The effects of ROCK2 haploinsufficiency were observed whether Th17 differentiation was driven by exposure to TGF-β and IL-6 (Figure 6, A–E) or by exposure to TGF-β and IL-21 (Figure 6, D and E). Production of IFN-γ and IL-4 by *Rock2*$^{+/-}$ T cells under Th17 conditions was slightly increased, an effect that was even more pronounced when cells were cultured under Th0 conditions (Figure 6E and Supplemental Figure 6A). Furthermore, no alteration in the expression of $Foxp3^+$ was observed under these culture conditions (Supplemental Figure 6B). ROCK2 haploinsufficiency did not impair the ability of naive T cells to differentiate into Th1 or Th2 cells (Supplemental Figure 6, C–E). Additionally, *Rock2*$^{+/-}$ $CD4^+$ T cells produced levels of IL-21 comparable to those of *Rock2*$^{+/+}$ $CD4^+$ T cells when cultured under Th2 differentiating conditions (Supplemental Figure 6E). Thus, ROCK2 haploinsufficiency selectively impaired the differentiation of naive $CD4^+$ T cells toward the Th17 lineage.

We next directly evaluated whether the diminished ability of *Rock2*$^{+/-}$ $CD4^+$ T cells to differentiate into Th17 cells was associated with defects in IRF4 phosphorylation and IRF4 function. *Rock2*$^{+/-}$ $CD4^+$ T cells differentiated under Th17 conditions exhibited decreased pIRF4 compared with *Rock2*$^{+/+}$ $CD4^+$ T cells (Figure 6F). ChIP assays were also conducted on *Rock2*$^{+/+}$ and *Rock2*$^{+/-}$ $CD4^+$ T cells stimulated under either Th0 or Th17 conditions; in WT $CD4^+$ T cells, IRF4 bound to the IL-17A, IL-21, and RORγt promoters under Th17, but not Th0, conditions (Figure 6G). Importantly, the ability of IRF4 to target the IL-17A, IL-21, and RORγt promoters under Th17 conditions was severely impaired in *Rock2*$^{+/-}$ $CD4^+$ cells. Since IRF4 can also regulate the production of IL-21 in Th2 cells (13), ChIP assays were also conducted on *Rock2*$^{+/-}$ $CD4^+$ cells cultured under Th2 conditions (Supplemental Figure 6F). Consistent with our finding that ROCK2 haploinsufficiency did not affect the production of IL-21 under Th2 conditions, binding of IRF4 to the IL-21 promoter was not altered in *Rock2*$^{+/-}$ $CD4^+$ cells cultured under these conditions. No effect of ROCK2 haploinsufficiency on IRF4 binding to the IL-10 promoter in Th2 cells was detected (Supplemental Figure 6F). Together, these results strongly support the notion that, in WT $CD4^+$ T cells, ROCK2 is activated upon exposure to Th17 skewing conditions, and that this step selectively regulates IRF4 function during Th17 differentiation.

ROCK inhibition decreases IL-17 and IL-21 levels in vivo and ameliorates arthritis in Def6$^{trap/trap}$*DO11.10 mice*. The involvement of ROCK2 in the regulation of IL-17 and IL-21 production suggested that inhibition of this kinase in vivo could be effective in diminishing the aberrant production of these cytokines that characterizes spontaneous autoimmune models such as the *Def6*$^{trap/trap}$DO11.10 mice (13). We thus administered Fasudil, which is more easily administered than Y27632 (50), to *Def6*$^{trap/trap}$DO11.10 mice starting at 8 weeks of age, prior to the onset of active disease. Fasudil-treated *Def6*$^{trap/trap}$DO11.10 mice developed significantly less severe arthritis and lower titers of rheumatoid factor (RF) than did controls (Figure 7, A and B). Fasudil treatment did not affect total splenic cellularity, expansion and activation of *Def6*$^{trap/trap}$DO11.10 $CD4^+$ T cells, or number of regulatory T cells (Supplemental Figure 7, A–D). However, Fasudil treatment markedly decreased the expansion of PNA^+ B cells, $sIgG1^+$ B cells, and $B220^{lo}CD138^+$ plasma cells in *Def6*$^{trap/trap}$DO11.10 mice (Supplemental Figure 7E). To assess whether the beneficial actions of Fasudil in *Def6*$^{trap/trap}$DO11.10 mice were linked to effects on IL-17 and IL-21 production, $CD4^+$ T cells were harvested from either treated or untreated *Def6*$^{trap/trap}$DO11.10 mice and restimulated in vitro. Fasudil treatment decreased the production of IL-17 and IL-21 by *Def6*$^{trap/trap}$DO11.10 $CD4^+$ T cells, but did not alter the cells' production of IL-2 (Figure 7C). ROCK inhibition was thus effective in reducing IL-17 and IL-21 levels in vivo and in preventing the spontaneous development of arthritis in *Def6*$^{trap/trap}$DO11.10 mice.

One of the major challenges in treating autoimmune disorders is that therapies need to be effective in downmodulating the function of previously activated $CD4^+$ T cells. The ability of ROCK inhibitors to interfere with the in vitro production of IL-17 and IL-21 by effector $CD4^+$ T cells suggested that ROCK inhibition could also be effective in *Def6*$^{trap/trap}$DO11.10 mice with established disease. Fasudil was thus administered to *Def6*$^{trap/trap}$DO11.10 mice in a treatment protocol starting at 14 weeks of age, once active disease had commenced. Whereas arthritis in untreated *Def6*$^{trap/trap}$DO11.10 mice worsened in severity over time, administration of Fasudil to *Def6*$^{trap/trap}$DO11.10 mice for 12 weeks suppressed disease progression and serum levels of RF (Figure 7, D and E). The beneficial effects of Fasudil treatment were accompanied by lower levels of IL-17 and IL-21 in the serum and diminished *Il17* and *Il21* transcript levels in the joints (Figure 7, F and G), although variability between individual mice prevented the decrease in *Il17* gene expression from achieving statistical significance. Consistent with previous studies (50), long-term treatment with Fasudil did not lead to any significant side effects. Thus, ROCK inhibition was effective in decreasing IL-17 and IL-21 production and ameliorating symptoms even during ongoing autoimmune responses.

Aberrant ROCK2 activation and IRF4 function in $CD4^+$ T cells from MRL/lpr mice. Deregulated production of IL-17 and IL-21 has been observed in a number of spontaneous mouse models of autoimmunity, including the lupus-prone MRL/lpr mouse (51, 52). We thus investigated whether aberrant ROCK2 activation also occurs in $CD4^+$ T cells from MRL/lpr mice. ROCK2 activity assays were performed on $CD4^+$ T cells from MRL/lpr mice that were either unstimulated or stimulated under neutral conditions, and ROCK2 immunoprecipitates from stimulated MRL/lpr $CD4^+$ T cells had higher pMYPT1 levels than did WT $CD4^+$ T cells (Figure 8A). Consistent with our findings in Def6-deficient $CD4^+$ T cells, the increased ROCK2 activation observed in stimulated MRL/lpr $CD4^+$ T cells was associated with enhanced IRF4 binding to the IL-21 promoter and with higher levels of pIRF4 (Figure 8, B and C). Furthermore, the enhanced production of IL-17 and IL-21 by MRL/lpr $CD4^+$ T cells was inhibited by the presence of either Y27632 or Fasudil (Figure 8D). Together, these results suggest that aberrant ROCK2 activation is not limited to Def6-deficient $CD4^+$ T cells, but is also present in $CD4^+$ T cells from MRL/lpr mice.

To test whether ROCK inhibition ameliorates autoimmunity in MRL/lpr mice, Fasudil was administered to MRL/lpr mice starting at 10 weeks of age for a period of 9 weeks. Fasudil did not exert any

significant effects on the splenomegaly and lymphadenopathy that develops in MRL/lpr mice (data not shown). Furthermore, Fasudil treatment did not correct the expansion or activation of $CD4^+$ T cells or alter the number of $CD3^+CD4^-CD8^-$ T cells observed in MRL/lpr mice (Supplemental Figure 8, A and B). However, consistent with our observations in *Def6*$^{trap/trap}$DO11.10 mice, Fasudil administration led to a marked reduction in IL-17 and IL-21 production in the spleen, which was associated with diminished expansion of $sIgG1^+$ B cells and plasma cells and with a marked decrease in dsDNA autoantibody production (Figure 8, E–G). The beneficial effects of Fasudil on humoral responses resulted in decreased glomerular deposition of IgG and C3 (Supplemental Figure 8, C and D) and significant amelioration of proteinuria (Figure 8H). Together, these data suggest that aberrant activation of ROCK2 in $CD4^+$ T cells, via its ability to regulate IRF4 function and IL-17 and IL-21 production, may play a broad role in the pathogenesis of autoimmunity.

Discussion

ROCKs are known to subserve key functions in endothelial cells and other nonhematopoietic cells (28–31); however, their role in the immune system, particularly in $CD4^+$ T cells, has been largely unexplored. In this report, we demonstrated that ROCK2 was physiologically activated when $CD4^+$ T cells were exposed to Th17 skewing conditions. We furthermore showed that ROCK2 phosphorylated IRF4, and that this event modulated the ability of IRF4 to bind to the IL-17 and IL-21 promoters and regulate production of these cytokines. Notably, we detected aberrant ROCK2 activation that led to deregulated IRF4 function in $CD4^+$ T cells from 2 distinct spontaneous mouse models of autoimmunity. Furthermore, ROCK inhibition effectively decreased IL-17 and IL-21 production in vivo and ameliorated ongoing autoimmune responses. Together, these data support a model whereby deregulated ROCK2 activation in $CD4^+$ T cells, via its ability to directly affect production of IL-17 and IL-21, may be an important pathogenic mechanism in the development of autoimmunity (Supplemental Figure 9).

Despite the well-known role of TGF-β in promoting the differentiation of Th17 cells, the signaling pathways used by TGF-β to regulate this process are largely unknown, since activation of Smad proteins does not appear to mediate the process (53, 54). Our findings indicate that exposure to TGF-β leads to the activation of ROCK2 in $CD4^+$ T cells, and that ROCK2 activation regulates Th17 differentiation. Indeed, interfering with ROCK2 function in WT $CD4^+$ T cells caused defective Th17 skewing, which supports the idea that ROCK2 activation by TGF-β plays an intrinsic role in the differentiation of Th17 cells. Furthermore, ROCK2 haploinsufficiency caused defective Th17 cell differentiation, whether naive $CD4^+$ T cells were cultured with TGF-β and IL-6 or with TGF-β and IL-21. Our present results thus support the notion that activation of ROCK2 constitutes an important step in the signaling cascade used by TGF-β to control Th17 cell development. Interestingly, reintroduction of a phosphomimetic form of IRF4 into IRF4-deficient $CD4^+$ T cells failed to generate IL-17–producing cells when these cells were cultured in the presence of IL-6 alone (P.S. Biswas, unpublished observations), which suggests that TGF-β needs to activate signaling events in addition to ROCK2 in order to implement the full Th17 differentiation program.

One of the key mechanisms by which ROCK2 controls the differentiation of Th17 cells is via phosphorylation of IRF4. Indeed, pIRF4 was detected in Th17 cells, but not in Th0 cells, and our mutational analysis demonstrated that this phosphorylation event was important for binding of IRF4 to the IL-17 and IL-21 promoters and for the differentiation of Th17 cells. Consistent with previous studies demonstrating that IRF4-deficient $CD4^+$ T cells cannot upregulate RORγt upon exposure to Th17 skewing conditions (11), IRF4 phosphorylation was also important for the ability of IRF4 to directly target the RORγt promoter and for the induction of RORγt. Interestingly, the 2 serines targeted by ROCK2, S446 and S447, are contained within an α-helical region of IRF4 located carboxyterminal of the IRF association domain (55). Structural studies of IRF3 and IRF5 have demonstrated that this region serves an autoinhibitory function and that its phosphorylation triggers a conformational rearrangement that relieves the autoinhibition (55–57). Despite sharing structural similarities, the carboxyterminal regions of different IRFs exhibit very low sequence similarity (55). It is thus not surprising that different kinases mediate the phosphorylation of distinct IRFs and that, unlike the case of IRF3 and IRF5, phosphorylation of IRF4 does not alter its ability to translocate to the nucleus, but rather regulates the ability of nuclear IRF4 to target selected DNA binding sites.

Although $CD4^+$ T cells from WT mice activated ROCK2 physiologically when exposed to Th17 skewing conditions, we found that $CD4^+$ T cells from Def6-deficient mice aberrantly activated ROCK2 under neutral conditions. Together with our previous studies (13), the present work supports the idea that the ability of Def6 to bind IRF4 as well as its capacity to control Rho GTPase-mediated pathways ultimately contribute to its role as a regulator of IL-17 and IL-21 production. Because IRF4 is induced upon T cell activation in all Th subsets, the multimodal regulation of IRF4 by Def6 may be critical to ensure that IRF4 upregulates both IL-17 and IL-21 only in the presence of specific inflammatory conditions. Remarkably, whereas ROCK2 haploinsufficiency impaired the function of IRF4 and the production of IL-21 under Th17 skewing conditions, it did not exert any effects on the ability of IRF4 to mediate the production of IL-21 by Th2 cells, which supports the idea that by use of a complex regulatory network, $CD4^+$ T cells can fine tune the production of these potentially pathogenic cytokines.

Intriguingly, a recent study has suggested that Def6 plays a positive role in Th17 differentiation (58). There are multiple, and not mutually exclusive, explanations for these seemingly contradictory results. Notably, the lack of Def6 exerts complex effects on T cell proliferation. Indeed, although hyperresponsive to low levels of stimulation, Def6-deficient T cells exhibit impaired proliferation under strong stimulatory conditions (13). This defective expansion, in turn, can broadly alter the ability of Def6-deficient T cells to acquire effector functions upon exposure to strong stimuli, as evidenced by the finding that Def6-deficient T cells exhibit defective differentiation not only toward the Th17 lineage, but also toward the Th1 and Th2 lineages (58, 59). Similar to $CD4^+$ T cells from many autoimmune patients, Def6-deficient T cells also exhibit impaired production of IL-2 (21, 59). Because IL-2 is known to inhibit Th17 differentiation (60), this relative decrease in IL-2 production is likely to play a role in the deregulated IL-17 production by these cells. Provision of exogenous IL-2 to Def6-deficient T cells (58) may thus also influence their ability to produce IL-17 and IL-21. We have furthermore proposed that, under strong inflammatory conditions, the ability of Def6 to constrain IRF4 should be inhibited, so that IRF4 can mediate the production of high levels of IL-17 and IL-21 (14). Thus, under Th17 skewing conditions, the role of Def6 in the regulation of other pathways, such as NFAT-mediated pathways (23, 59), may become more prominent.

Although we initially delineated the importance of the ROCK2-IRF4 axis in the production of IL-17 and IL-21 by exploring the mechanisms that go awry in Def6-deficient CD4+ T cells, aberrant activation of this pathway can also be detected in CD4+ T cells from another spontaneous model of autoimmunity, the MRL/lpr mouse. Interestingly, we recently observed that this pathway was also deregulated in CD4+ T cells from NOD mice (P.S. Biswas, unpublished observations), another mouse model in which spontaneous autoimmunity is highly dependent on the presence of IL-21 (61–63). The mechanisms underlying the aberrant activation of ROCK2 in these additional models are unclear at present. TCR engagement, however, has previously been shown to lead to both Rac and RhoA activation (25, 64). Given the ability of Rac to inhibit RhoA, one plausible explanation is that in MRL/lpr and NOD mice, the TCR signaling pathway leading to Rac activation is diminished (e.g., because of dysfunction in Def6 and/or other components of this pathway), leading to stronger and/or more prolonged RhoA activation. Additional defects, such as failure of IRF4 phosphorylation to mediate a negative feedback loop on ROCK2 activation, may also exist. Furthermore, administration of Fasudil to proteolipid protein–immunized SJL/J mice has been shown to ameliorate the development of EAE (65), which suggests that ROCK activation may also play a pathogenic role in induced models of autoimmunity. It is also important to note that ROCK activation has been observed in both RA and SLE patients (34, 66). Together, these findings suggest that deregulated activation of this pathway may be a common pathogenic mechanism in the development of autoimmunity.

Our present results support the idea that the capacity of ROCK inhibitors to interfere with the production of IL-17 and IL-21 by CD4+ T cells is a critical component of the beneficial effects of Fasudil on the autoimmune responses observed in both Def6-deficient and MRL/lpr mice. In particular, the finding that ROCK inhibition was effective in diminishing the production of IL-17 and IL-21 by effector T cells and in ameliorating ongoing autoimmune responses could have profound clinical implications. Interestingly, our pharmacological and genetic manipulations indicated that blocking the ability of ROCK2 to phosphorylate IRF4 decreases, but does not abolish, the production of IL-17 and IL-21, which suggests that targeting this step may ameliorate the inappropriate production of these pathogenic cytokines without simultaneously causing profound immunosuppression. The remarkable selectivity for the ROCK2-mediated phosphorylation of IRF4 in controlling IL-21 production only in specific settings may further attest to this idea. Interestingly, inhibition of ROCKs has also been linked to the pleiotropic effects of statins (36, 67). Since statins have previously been shown to inhibit IL-17 production and RORγt expression (68), some of their antiinflammatory effects may be caused by the ability of statins to interfere with the ROCK2-mediated phosphorylation of IRF4.

In contrast to our findings in CD4+ T cells, aberrant ROCK activation was not observed in either B cells or myeloid cells from Def6-deficient mice, and we did not detect any direct effect of ROCK inhibitors on B cell responses in vitro (Supplemental Figure 10, A and B). However, we cannot exclude that aberrant activation of ROCKs in other cellular compartments also contributes to autoimmune symptomatology. Indeed, increased ROCK activity has been linked to the production of proinflammatory cytokines by synovial fibroblasts (66), raising the possibility that deregulated activation of ROCKs in multiple cellular compartments can help generate a milieu that favors the development of autoimmune responses. In this respect, it is interesting to note that aberrant activation of ROCKs has previously been implicated in endothelial dysfunction and cardiovascular disease (30, 31). Because many patients with RA and SLE exhibit an increased risk of developing premature cardiovascular disease (69, 70), our studies raise the intriguing possibility that the aberrant autoimmune responses and the vascular dysfunction observed in these patients may share a common mechanistic link.

Although nonselective ROCK inhibitors like Fasudil have demonstrated efficacy and a good safety profile in patients for the treatment of cardiovascular disorders (36, 37), our studies indicate that regulation of IL-17 and IL-21 is a ROCK2-specific effect, which supports the idea that development of compounds selectively targeting ROCK2 may represent an important treatment modality for RA, SLE, and possibly other autoimmune disorders characterized by enhanced IL-17 and IL-21 production. Thus, a better understanding of the regulation of transcriptional complexes controlling IL-17 and IL-21 could lead to the emergence of effective therapies for the treatment of autoimmune diseases.

Methods

Mice. Def6-deficient mice were generated by Lexicon Pharmaceuticals (Omnibank) using a gene trapping strategy, and are thus referred to herein as *Def6*$^{trap/trap}$ mice. These mice were backcrossed into either Balb/c or C57BL/6 mice for more than 10 generations. *Def6*$^{trap/trap}$ mice on a Balb/c background were then crossed to DO11.10 TCR transgenic mice (Jackson Laboratory) to generate *Def6*$^{trap/trap}$DO11.10 mice, as described previously (13). *Irf4*$^{-/-}$ mice on a C57BL/6 background were obtained from T. Mak (University of Toronto and Amgen Institute, Toronto, Ontario, Canada; ref. 71). To generate *Def6*$^{trap/trap}$*Irf4*$^{-/-}$ mice, *Irf4*$^{-/-}$ mice were crossed with *Def6*$^{trap/trap}$ mice that had been backcrossed onto the C57BL/6 background, as described previously (13). *Rock2*$^{+/-}$ mice backcrossed on a C57BL/6 background for more than 10 generations were generated as previously described (48). MRL/lpr mice were obtained from Jackson Laboratories. All mice used in the experiments were kept under specific pathogen–free conditions. The experimental protocols were approved by the Institutional Animal Care and Use Committee of Columbia University.

Flow cytometry. Single-cell suspensions from thymus, spleen, and lymph nodes were isolated; stained with fluorochrome-conjugated CD3e, CD4, CD5, CD8, B220, CD25, CD44, CD62L, CD69, CD138, IgG1, CD11b (Pharmingen), ICOS Abs (eBiosciences), and PNA (Jackson ImmunoResearch Laboratories Inc.); and analyzed by FACS. Data were analyzed using FlowJo (Treestar) software. Intracellular staining of pERM was performed as previously described (72) using anti-pERM Ab (Cell Signaling) followed by anti-rabbit Alexa Fluor 488 (Invitrogen) as secondary Ab. Intracellular staining of IL-17 and IFN-γ was performed as previously described (13).

In vivo Fasudil studies. For the *Def6*$^{trap/trap}$DO11.10 mouse preventive protocol, 8-week-old female *Def6*$^{trap/trap}$DO11.10 mice (n = 10 per group) were fed Fasudil in drinking water (100 mg/kg) as previously described (50), or left untreated, for 10 weeks. Age- and sex-matched *Def6*$^{+/+}$DO11.10 mice (n = 10) were used as controls. Animals were grouped based on RF levels to ensure similar levels of autoantibodies in the treated and untreated animals. During the course of study, mice were weighed to ensure equivalent water intake by the treated and untreated groups. Mice were scored for arthritis every 7 days as previously described (13). Serum was collected every 14 days.

For the *Def6*$^{trap/trap}$DO11.10 mouse treatment protocol, 14-week-old female *Def6*$^{trap/trap}$DO11.10 mice were fed Fasudil in drinking water (100 mg/kg), or left untreated, for 12 weeks (n = 7 per group). Animals were grouped based on arthritis score and RF levels to ensure similar levels of autoan-

tibodies in the treated and untreated animals. During the course of the study, mice were weighed to ensure equivalent water intake by the treated and untreated groups. Mice were scored for arthritis every 7 days as previously described (13). Serum was collected every 14 days.

For the MRL/lpr mouse protocol, 10-week-old female MRL/lpr mice were fed Fasudil in drinking water (100 mg/kg), or left untreated, for 9 weeks (n = 7 per group). Proteinuria was measured every 7 days by dipstick analysis. Serum was collected every 14 days.

Histopathology, immunohistochemical, and immunofluorescence staining. Tissue specimens were fixed in 10% neutral buffered formalin and embedded in paraffin. Tissue sections were stained with H&E and analyzed by light microscopy. Glomerulonephritis severity was assessed as previously described (73). Joints were fixed in 10% phosphate-buffered formalin, decalcified in 10% EDTA-4Na, and embedded in paraffin. Immunofluorescence analysis on frozen kidney sections was performed by staining with FITC-labeled goat anti-mouse IgG or anti-C3 (Jackson ImmunoResearch Laboratories Inc.), and specimens were analyzed with a Zeiss LSM 510 laser scanning confocal microscope. The severity of immune complex deposition was determined in a blinded manner according to previously described parameters (73).

Serum autoantibodies. Serum levels of RF and dsDNA were determined by ELISA (Alpha Diagnostics for RF and dsDNA Abs) as described previously (13, 21).

CD4$^+$ T cell isolation and cytokine production. CD4$^+$ T cells were purified using the CD4$^+$ isolation kit from Miltenyi Biotech. For cytokine analysis, 1×10^6 cells/ml were stimulated with plate-bound anti-CD3ε and soluble anti-CD28 for 3 days and then rested in IL-2 for 4 days. Cells (1×10^6 cells/ml) were then restimulated by plate-bound anti-CD3ε and soluble anti-CD28 for 2 days. For Th17 differentiation studies, naive CD4$^+$ T cells were purified by sorting CD44^{lo}CD62L^{hi}CD25$^-$CD4$^+$ T cells, which were then activated by plate-bound anti-CD3ε and soluble anti-CD28 in the presence of anti–IFN-γ (10 μg/ml, BD Biosciences), anti–IL-4 (10 μg/ml, BD Biosciences), TGF-β (5 ng/ml, Peprotech), and either IL-6 (20 ng/ml, Peprotech) or IL-21 (50 ng/ml, R&D), as previously described (13). Supernatants were analyzed for IL-21 (R&D Systems), IL-17, IL-2, IL-4, and IFN-γ (eBioscience) production by ELISA. IL-2 (20 ng/ml) was added in the experiments shown in Figure 5D. Th1 and Th2 differentiation studies were conducted as previously described (13, 21).

Retroviral transduction. The retroviral constructs for DN-ROCK2 (provided by K. Kaibuchi, Nagoya University, Nagoya, Japan; ref. 42) and DN-RhoA (N19 Human RhoA; Addgene; refs. 43, 44) were generated by cloning the appropriate coding segment into the pGC–IRES–yellow fluorescent protein retroviral vector (YFP-RV) and the MSCV-IRES-GFP retroviral vector (GFP-RV), respectively. 293T cells were cotransfected with the retroviral plasmids together with the packaging vector pCL-Eco. After 72 hours, the retroviral supernatants were harvested, supplemented with 10 μg/ml polybrene, and used to twice infect naive CD4$^+$ T cells that had been stimulated for 24 hours. After the second infection, T cells were rested in IL-2 for 4 days before they were sorted for YFP$^+$ or GFP$^+$ cells. Sorted cells were checked for purity and restimulated with anti-CD3 and anti-CD28 for 48 hours. Supernatants were collected after 48 hours of stimulation for ELISA.

In vitro B cell assays. B cells were purified from mice by positive selection using CD45R microbeads (Miltenyi Biotech). B cell assays were performed as previously described (74). Briefly, B cells (10^5 cells/well) were stimulated with anti-IgM (10 μg/ml; Jackson ImmunoResearch) and anti-CD40 (5 μg/ml; BD Biosciences — Pharmingen) for 96 hours in the presence or absence of recombinant murine IL-21 (50 ng/ml; R&D Systems) and different doses of ROCK inhibitors as indicated. For proliferation assays, cultures were pulsed with [^{3}H]-thymidine (1 μCi/well; PerkinElmer) for the last 12 hours of culture. In vitro differentiation of plasma cells was determined by FACS after staining with a CD138 Ab (BD Biosciences — Pharmingen).

Cell extracts and Western blotting. Nuclear and cytoplasmic extracts were prepared using the NE-PER Nuclear and Cytoplasmic extraction reagent kit as previously described (75). ROCK1, ROCK2, and IRF4 Abs (Santa Cruz Biotechnology) were used to probe the blots according to the manufacturer's instructions. The purity of the nuclear and cytoplasmic fractions was verified by probing with Abs against Lamin B (Santa Cruz Biotechnology) and β-tubulin (Sigma-Aldrich). Rabbit polyclonal Ab specific for pIRF4 was generated by 21st Century Biochemicals Inc. using a synthetic phosphopeptide (YHRSIRH[pS][pS]IQE) corresponding to aa 439–450 of human IRF4 as an immunogen (IRF4 numbering based on GenBank accession no. U52682).

Real-time RT-PCR. Total RNA was isolated from cells or organs using RNeasy Mini Kit (Qiagen GmbH). cDNAs were prepared and analyzed for expression of the gene of interest by real-time PCR using a Sybr-Green PCR master mix kit (Applied Biosystems). Primers for IL-17, IL-21, and RORγt have been previously described (13). Primers for ROCK1 and ROCK2 were purchased from Quantitect Primer Assay (Qiagen). The expression of each gene was normalized to that of β-actin.

ChIP assays. ChIP assays were performed as previously described (13). Briefly, CD4$^+$ T cells were purified from WT and *Def6$^{trap/trap}$* mice and either left unstimulated or stimulated for 48 hours under unskewed conditions. After harvesting, cells were crosslinked with formaldehyde, and chromatin extracts were prepared by standard methods. The DNA/protein complexes were immunoprecipitated with an IRF4-specific or a control Ab. After crosslinking was reversed and proteins digested, the DNA was purified from the immunoprecipitates as well as from input extracts, and then analyzed by quantitative PCR using primers specific for the murine IL-21 promoter, as previously described (13), murine IL-17A promoter (forward, GGGCAAGGGATGCTCTCTAG; reverse, CTGAAGCTGCTGCAGAGCTG), murine RORγt promoter (forward, AAGCTCCCCAGCTAGAACTC; reverse, CCAGAGGTGCATTGGGTATG), and murine IL-10 promoter (forward, CGTGATGGAAGAATTAAAGAGAGTGA; reverse, CACCTTAGCACTCAGTTACCCAAA).

ONP assays. ONP assays were conducted as previously described (13). Briefly, nuclear extracts were precleared with streptavidin-agarose beads and then incubated with trimerized biotinylated double-stranded oligonucleotide corresponding to the IRF4 binding site within the IL-21 promoter (5′-CCTTGGTGAATGCTGAAAACTGGAATTCACCCAT-3′). Proteins bound to the biotin-labeled DNA were collected by streptavidin-agarose beads, separated by 8% SDS-PAGE, and analyzed by Western blotting using an IRF4 Ab (Santa Cruz Biotechnology).

ROCK2 kinase assays. ROCK2-mediated IRF4 phosphorylation was assessed by in vitro ROCK2 kinase assay using recombinant active ROCK2 kinase (Cell Signaling Technology) and immunoprecipitated myc epitope–tagged IRF4ΔDBD. Briefly, immunoprecipitated myc-IRF4ΔDBD was incubated with 50 ng purified active ROCK2 in 30 μl 1× kinase buffer (25 mM Tris, pH 7.5; 10 mM $MgCl_2$; 5 mM β-glycerolphosphate; 0.1 mM Na_3VO_4; and 2 mM DTT) containing 1 μM cold ATP and 10 μCi of [γ-^{32}P]ATP for 30 minutes at 30°C. The kinase reactions were terminated by adding SDS-PAGE sample buffer and boiling. The reaction samples were resolved on a 10% SDS-polyacrylamide gel. The gel was fixed, dried, and then autoradiographed to visualize the phosphorylated products. For the ROCK2 kinase activity assays, which use MYPT1 as the substrate (38), ROCK2 was first immunoprecipitated from extracts of purified CD4$^+$ T cells using an anti-ROCK2 Ab (Santa Cruz Biotechnology). The immunoprecipitated ROCK2 was then subjected to an in vitro kinase reaction by incubating with purified rMYPT1 substrate according to the manufacturer's instructions (Cell Biolabs). Levels of pMYPT1 by immunoprecipitated ROCK2 were detected by Western blotting using an anti-pMYPT1(T696) Ab.

Statistics. Results are expressed as mean ± SD. Differences between groups were calculated for statistical significance using 2-tailed unpaired Student's *t* test and Mann-Whitney *U* test. A *P* value less than 0.05 was considered significant.

Acknowledgments

We thank C. Schindler and Hua Gu for their critical reading of the manuscript and discussions. We thank K. Kaibuchi of Nagoya University for the gift of the DN-ROCK2 construct. We thank Mary Ann Gawinowicz from the Protein Core facility at Columbia University for her assistance with the mass spectrometry analysis. The research was supported by the Alliance for Lupus Research and by NIH grants HL62215 (A. Pernis) and HL052233 (J. Liao).

Received for publication March 3, 2010, and accepted in revised form June 30, 2010.

Address correspondence to: Alessandra B. Pernis, Autoimmunity and Inflammation Program, Hospital for Special Surgery, Caspary Research Building, Rm. 318, 535 East 70th Street, New York, New York 10021, USA. Phone: 212.606.1612; Fax: 212.717.1192; E-mail: pernisa@hss.edu.

Partha S. Biswas's, Sanjay Gupta's, Li Song's, Roslynn A. Stirzaker's, and Alessandra B. Pernis's present address is: Autoimmunity and Inflammation Program, Hospital for Special Surgery, New York, New York, USA.

1. Ettinger R, Kuchen S, Lipsky PE. The role of IL-21 in regulating B-cell function in health and disease. *Immunol Rev*. 2008;223:60–86.
2. Garrett-Sinha LA, John S, Gaffen SL. IL-17 and the Th17 lineage in systemic lupus erythematosus. *Curr Opin Rheumatol*. 2008;20(5):519–525.
3. Nalbandian A, Crispin JC, Tsokos GC. Interleukin-17 and systemic lupus erythematosus: current concepts. *Clin Exp Immunol*. 2009;157(2):209–215.
4. Spolski R, Leonard WJ. Interleukin-21: basic biology and implications for cancer and autoimmunity. *Annu Rev Immunol*. 2008;26:57–79.
5. Tesmer LA, Lundy SK, Sarkar S, Fox DA. Th17 cells in human disease. *Immunol Rev*. 2008;223:87–113.
6. Weaver CT, Hatton RD, Mangan PR, Harrington LE. IL-17 family cytokines and the expanding diversity of effector T cell lineages. *Annu Rev Immunol*. 2007;25:821–852.
7. Bettelli E, Korn T, Oukka M, Kuchroo VK. Induction and effector functions of T(H)17 cells. *Nature*. 2008;453(7198):1051–1057.
8. Dong C. TH17 cells in development: an updated view of their molecular identity and genetic programming. *Nat Rev Immunol*. 2008;8(5):337–348.
9. Takatori H, Kanno Y, Chen Z, O'Shea JJ. New complexities in helper T cell fate determination and the implications for autoimmune diseases. *Mod Rheumatol*. 2008;18(6):533–541.
10. Zhou L, Chong MM, Littman DR. Plasticity of CD4+ T cell lineage differentiation. *Immunity*. 2009;30(5):646–655.
11. Brustle A, et al. The development of inflammatory T(H)-17 cells requires interferon-regulatory factor 4. *Nat Immunol*. 2007;8(9):958–966.
12. Huber M, et al. IRF4 is essential for IL-21-mediated induction, amplification, and stabilization of the Th17 phenotype. *Proc Natl Acad Sci U S A*. 2008;105(52):20846–20851.
13. Chen Q, et al. IRF-4 Binding Protein inhibits interleukin-17 and interleukin-21 production by controlling the activity of IRF-4 transcription factor. *Immunity*. 2008;29(6):899–911.
14. Biswas P, Bhagat G, Pernis AB. IRF4 and its regulators: evolving insights into the pathogenesis of inflammatory arthritis? *Immunol Rev*. 2010;233(1):79–96.
15. Ahyi AN, Chang HC, Dent AL, Nutt SL, Kaplan MH. IFN regulatory factor 4 regulates the expression of a subset of Th2 cytokines. *J Immunol*. 2009;183(3):1598–1606.
16. Rengarajan J, Mowen KA, Mcbride KD, Smith ED, Singh H, Glimcher LH. Interferon regulatory factor 4 (IRF4) interacts with NFATc2 to modulate interleukin 4 gene expression. *J Exp Med*. 2002;195(8):1003–1012.
17. Hiscott J. Convergence of the NF-kappaB and IRF pathways in the regulation of the innate antiviral response. *Cytokine Growth Factor Rev*. 2007; 18(5-6):483–490.
18. Gupta S, et al. Molecular cloning of IBP, a SWAP-70 homologous GEF, which is highly expressed in the immune system. *Hum Immunol*. 2003;64(4):389–401.
19. Hotfilder M, Baxendale S, Cross MA, Sablitzky F. Def-2, -3, -6, -8, novel mouse genes differentially expressed in the hematopoietic system. *Br J Haematol*. 1999;106(2):335–344.
20. Tanaka Y, et al. SWAP-70-like adapter of T cells, an adapter protein that regulates early TCR-initiated signaling in Th2 lineage cells. *Immunity*. 2003;18(3):403–414.
21. Fanzo JC, et al. Loss of IRF-4-binding protein leads to the spontaneous development of systemic autoimmunity. *J Clin Invest*. 2006;116(3):703–714.
22. Gupta S, et al. T cell receptor engagement leads to the recruitment of IBP, a novel guanine nucleotide exchange factor, to the immunological synapse. *J Biol Chem*. 2003;278(44):43541–43549.
23. Becart S, Balancio AJ, Charvet C, Feau S, Sedwick CE, Altman A. Tyrosine-phosphorylation-dependent translocation of the SLAT protein to the immunological synapse is required for NFAT transcription factor activation. *Immunity*. 2008;29(5):704–719.
24. Heasman SJ, Ridley AJ. Mammalian Rho GTPases: new insights into their functions from in vivo studies. *Nat Rev Mol Cell Biol*. 2008;9(9):690–701.
25. Tybulewicz VL, Henderson RB. Rho family GTPases and their regulators in lymphocytes. *Nat Rev Immunol*. 2009;9(9):630–644.
26. Burridge K, Wennerberg K. Rho and Rac take center stage. *Cell*. 2004;116(2):167–179.
27. Ocana-Morgner C, Wahren C, Jessberger R. SWAP-70 regulates RhoA/RhoB-dependent MHCII surface localization in dendritic cells. *Blood*. 2009;113(7):1474–1482.
28. Riento K, Ridley AJ. Rocks: multifunctional kinases in cell behaviour. *Nat Rev Mol Cell Biol*. 2003;4(6):446–456.
29. Wettschureck N, Offermanns S. Rho/Rho-kinase mediated signaling in physiology and pathophysiology. *J Mol Med*. 2002;80(10):629–638.
30. Noma K, Oyama N, Liao JK. Physiological role of ROCKs in the cardiovascular system. *Am J Physiol Cell Physiol*. 2006;290(3):C661–C668.
31. Loirand G, Guerin P, Pacaud P. Rho kinases in cardiovascular physiology and pathophysiology. *Circ Res*. 2006;98(3):322–334.
32. Lee JH, Katakai T, Hara T, Gonda H, Sugai M, Shimizu A. Roles of p-ERM and Rho-ROCK signaling in lymphocyte polarity and uropod formation. *J Cell Biol*. 2004;167(2):327–337.
33. Smith A, Bracke M, Leitinger B, Porter JC, Hogg N. LFA-1-induced T cell migration on ICAM-1 involves regulation of MLCK-mediated attachment and ROCK-dependent detachment. *J Cell Sci*. 2003;116(pt 15):3123–3133.
34. Li Y, et al. Phosphorylated ERM is responsible for increased T cell polarization, adhesion, and migration in patients with systemic lupus erythematosus. *J Immunol*. 2007;178(3):1938–1947.
35. Tharaux PL, et al. Rho kinase promotes alloimmune responses by regulating the proliferation and structure of T cells. *J Immunol*. 2003;171(1):96–105.
36. Liao JK, Seto M, Noma K. Rho kinase (ROCK) inhibitors. *J Cardiovasc Pharmacol*. 2007;50(1):17–24.
37. Olson MF. Applications for ROCK kinase inhibition. *Curr Opin Cell Biol*. 2008;20(2):242–248.
38. Mong PY, Wang Q. Activation of Rho kinase isoforms in lung endothelial cells during inflammation. *J Immunol*. 2009;182(4):2385–2394.
39. Tran Quang C, Gautreau A, Arpin M, Treisman R. Ezrin function is required for ROCK-mediated fibroblast transformation by the Net and Dbl oncogenes. *EMBO J*. 2000;19(17):4565–4576.
40. Tanaka T, et al. Nuclear Rho kinase, ROCK2, targets p300 acetyltransferase. *J Biol Chem*. 2006; 281(22):15320–15329.
41. Hu CM, Jang SY, Fanzo JC, Pernis AB. Modulation of T cell cytokine production by interferon regulatory factor-4. *J Biol Chem*. 2002;277(51):49238–49246.
42. Amano M, Chihara K, Nakamura N, Kaneko T, Matsuura Y, Kaibuchi K. The COOH terminus of Rho-kinase negatively regulates rho-kinase activity. *J Biol Chem*. 1999;274(45):32418–32424.
43. Qiu RG, Chen J, Kirn D, McCormick F, Symons M. An essential role for Rac in Ras transformation. *Nature*. 1995;374(6521):457–459.
44. Qiu RG, Chen J, McCormick F, Symons M. A role for Rho in Ras transformation. *Proc Natl Acad Sci U S A*. 1995;92(25):11781–11785.
45. Lai JM, Hsieh CL, Chang ZF. Caspase activation during phorbol ester-induced apoptosis requires ROCK-dependent myosin-mediated contraction. *J Cell Sci*. 2003;116(pt 17):3491–3501.
46. Zhang YE. Non-Smad pathways in TGF-beta signaling. *Cell Res*. 2009;19(1):128–139.
47. Thumkeo D, et al. Targeted disruption of the mouse rho-associated kinase 2 gene results in intrauterine growth retardation and fetal death. *Mol Cell Biol*. 2003;23(14):5043–5055.
48. Noma K, et al. ROCK1 mediates leukocyte recruitment and neointima formation following vascular injury. *J Clin Invest*. 2008;118(5):1632–1644.
49. Yamaguchi H, Kasa M, Amano M, Kaibuchi K, Hakoshima T. Molecular mechanism for the regulation of rho-kinase by dimerization and its inhibition by fasudil. *Structure*. 2006;14(3):589–600.
50. Hattori T, et al. Long-term inhibition of Rho-kinase suppresses left ventricular remodeling after myocardial infarction in mice. *Circulation*. 2004;109(18):2234–2239.
51. Herber D, Brown TP, Liang S, Young DA, Collins M, Dunussi-Joannopoulos K. IL-21 has a pathogenic role in a lupus-prone mouse model and its blockade with IL-21R.Fc reduces disease progression. *J Immunol*. 2007;178(6):3822–3830.
52. Zhang Z, Kyttaris VC, Tsokos GC. The role of IL-23/IL-17 axis in lupus nephritis. *J Immunol*. 2009;183(5):3160–3169.
53. Yang XO, et al. Molecular antagonism and plasticity of regulatory and inflammatory T cell programs.

Immunity. 2008;29(1):44–56.
54. Martinez GJ, et al. SMAD3 differentially regulates the induction of regulatory and inflammatory T cell differentiation. *J Biol Chem*. 2009; 284(51):35283–35286.
55. Chen W, et al. Insights into interferon regulatory factor activation from the crystal structure of dimeric IRF5. *Nat Struct Mol Biol*. 2008;15(11):1213–1220.
56. Qin BY, et al. Crystal structure of IRF-3 reveals mechanism of autoinhibition and virus-induced phosphoactivation. *Nat Struct Biol*. 2003;10(11):913–921.
57. Takahasi K, et al. X-ray crystal structure of IRF-3 and its functional implications. *Nat Struct Biol*. 2003;10(11):922–927.
58. Canonigo-Balancio AJ, Fos C, Prod'homme T, Becart S, Altman A. SLAT/Def6 plays a critical role in the development of Th17 cell-mediated experimental autoimmune encephalomyelitis. *J Immunol*. 2009;183(11):7259–7267.
59. Becart S, et al. SLAT regulates Th1 and Th2 inflammatory responses by controlling Ca2+/NFAT signaling. *J Clin Invest*. 2007;117(8):2164–2175.
60. Laurence A, et al. Interleukin-2 signaling via STAT5 constrains T helper 17 cell generation. *Immunity*. 2007;26(3):371–381.
61. Datta S, Sarvetnick NE. IL-21 limits peripheral lymphocyte numbers through T cell homeostatic mechanisms. *PLoS One*. 2008;3(9):e3118.
62. Spolski R, Kashyap M, Robinson C, Yu Z, Leonard WJ. IL-21 signaling is critical for the development of type I diabetes in the NOD mouse. *Proc Natl Acad Sci U S A*. 2008;105(37):14028–14033.
63. Sutherland AP, et al. Interleukin-21 is required for the development of type 1 diabetes in NOD mice. *Diabetes*. 2009;58(5):1144–1155.
64. Pernis AB. Rho GTPase-mediated pathways in mature CD4+ T cells. *Autoimmun Rev*. 2009; 8(3):199–203.
65. Sun X, et al. The selective Rho-kinase inhibitor Fasudil is protective and therapeutic in experimental autoimmune encephalomyelitis. *J Neuroimmunol*. 2006;180(1-2):126–134.
66. He Y, et al. Antiinflammatory effect of Rho kinase blockade via inhibition of NF-kappaB activation in rheumatoid arthritis. *Arthritis Rheum*. 2008;58(11):3366–3376.
67. Abeles AM, Pillinger MH. Statins as antiinflammatory and immunomodulatory agents: a future in rheumatologic therapy? *Arthritis Rheum*. 2006;54(2):393–407.
68. Zhang X, Jin J, Peng X, Ramgolam VS, Markovic-Plese S. Simvastatin inhibits IL-17 secretion by targeting multiple IL-17-regulatory cytokines and by inhibiting the expression of IL-17 transcription factor RORC in CD4+ lymphocytes. *J Immunol*. 2008; 180(10):6988–6996.
69. Libby P. Role of inflammation in atherosclerosis associated with rheumatoid arthritis. *Am J Med*. 2008; 121(10 suppl 1):S21–31.
70. Roman MJ, Salmon JE. Cardiovascular manifestations of rheumatologic diseases. *Circulation*. 2007; 116(20):2346–2355.
71. Mittrucker H, et al. Requirement for the transcription factor LSIRF/IRF4 for mature B and T lymphocyte function. *Science*. 1997;275(5299):540–543.
72. Garcia GG, Sadighi Akha AA, Miller RA. Age-related defects in moesin/ezrin cytoskeletal signals in mouse CD4 T cells. *J Immunol*. 2007;179(10):6403–6409.
73. Atkinson C, Qiao F, Song H, Gilkeson GS, Tomlinson S. Low-dose targeted complement inhibition protects against renal disease and other manifestations of autoimmune disease in MRL/lpr mice. *J Immunol*. 2008;180(2):1231–1238.
74. Kuchen S, et al. Essential role of IL-21 in B cell activation, expansion, and plasma cell generation during CD4+ T cell-B cell collaboration. *J Immunol*. 2007;179(9):5886–5896.
75. So T, Song J, Sugie K, Altman A, Croft M. Signals from OX40 regulate nuclear factor of activated T cells c1 and T cell helper 2 lineage commitment. *Proc Natl Acad Sci U S A*. 2006;103(10):3740–3745.